



Published in final edited form as:

Nat Genet. 2017 April ; 49(4): 515–526. doi:10.1038/ng.3792.

Targeted sequencing identifies 91 neurodevelopmental disorder risk genes with autism and developmental disability biases

A full list of authors and affiliations appears at the end of the article.

Abstract

Gene-disruptive mutations contribute to the biology of neurodevelopmental disorders (NDDs), but most pathogenic genes are not known. We sequenced 208 candidate genes from >11,730 patients and >2,867 controls. We report 91 genes with an excess of *de novo* mutations or private disruptive mutations in 5.7% of patients, including 38 novel NDD genes. *Drosophila* functional assays of a subset bolster their involvement in NDDs. We identify 25 genes that show a bias for autism versus intellectual disability and highlight a network associated with high-functioning autism (FSIQ>100). Clinical follow-up for *NAA15*, *KMT5B*, and *ASH1L* reveals novel syndromic and non-syndromic forms of disease.

Neurodevelopmental disorders (NDDs) are a heterogeneous collection of psychiatric and clinical diagnoses that encompass autism spectrum disorders (ASD), intellectual disability/developmental delay (ID/DD), attention-deficit/hyperactivity, motor and tic disorders, and language communication disorders¹. Although each diagnosis is distinctive based on the Diagnostic and Statistical Manual of Mental Disorders, 5th edition (DSM-5)¹, NDDs often co-occur. Twin studies have shown that NDDs have a heritable component². In addition to phenotypic overlaps, copy number variant (CNV) studies have shown that risk genotypes

Users may view, print, copy, and download text and data-mine the content in such documents, for the purposes of academic research, subject always to the full Conditions of use: http://www.nature.com/authors/editorial_policies/license.html#terms

Corresponding author: Evan E. Eichler, Ph.D., Department of Genome Sciences, University of Washington School of Medicine, Foegen S-413A, Box 355065, 3720 15th Ave NE, Seattle, WA 98195-5065, eee@gs.washington.edu, Tel 001-(1)2066857336, Fax 001-(1)2062215795.

^αPresent address: Department of Pharmacology, Creighton University School of Medicine, Omaha, NE, USA.

^ψShared first authors.

^βAuthors contributed equally.

DATA AVAILABILITY

The smMIP sequencing data for this study can be downloaded from the NIMH data repository National Database for Autism Research (NDAR) at <http://dx.doi.org/10.5072/1324821> and is available to all qualified researchers after data use certification. The URLs for data utilized herein are as follows: NHLBI Exome Sequencing Project (ESP) Exome Variant Server, <http://evs.gs.washington.edu/EVS/>; UCSC Genome Browser, <http://genome.ucsc.edu/>; MIPgen, <http://shendurelab.github.io/MIPGEN/>; CADD Score, <http://cadd.gs.washington.edu/>; NCBI Gene, <http://www.ncbi.nlm.nih.gov/gene/>; Exome Aggregation Consortium (ExAC), <http://exac.broadinstitute.org/>.

AUTHOR CONTRIBUTIONS

E.E.E., H.A.F.S., B.X., and B.P.C. designed the study; H.A.F.S., B.X., T.W., K.H., L.V., and J.L. performed the experiments; B.P.C. helped with smMIP design and data analysis; F.H. performed the gene network analysis; R.A.B., J.G., and S.T. analyzed the patient data; B.X., M.F., B.H., and A.C.N. performed and analyzed the *Drosophila* data; other authors participated in the sample collection and DNA extraction and/or preparation. E.E.E., H.A.F.S., B.P.C., B.X., A.S., M.F., and R.A.B. wrote the manuscript with input from all authors.

CONFLICT OF INTERESTS

E.E.E. is on the scientific advisory board (SAB) of DNAnexus, Inc. and was an SAB member of Pacific Biosciences, Inc. (2009–2013) and SynapDx Corp. (2011–2013); E.E.E. is a consultant for Kunming University of Science and Technology (KUST) as part of the 1000 China Talent Program.

overlap between NDDs³. While these data strongly suggest that common genetic etiologies underlie a subset of broadly defined NDDs, there has been criticism that gene discovery efforts have failed to distinguish ID/DD genes from those contributing to ASD without ID⁴.

Large numbers of potentially pathogenic mutations have been identified based on exome sequencing of NDD cohorts, but in most cases only a single occurrence of a DN mutation in a particular gene has been discovered. Significantly larger numbers of cases and controls are required to prove the statistical significance of individual genes. Leveraging samples and data from multiple comorbid conditions, in principle, can increase our sensitivity to identify risk genes. Phenotypic follow-up of cases broadly drawn from NDDs has previously allowed us to explore specific clinical phenotypes in a genotype-first manner⁵, such as in the case of genes like *CHD8*⁶, *DYRK1A*⁷, and *ADNP*⁸.

Using single-molecule molecular inversion probes (smMIPs)^{9,10}, we sequenced the coding and splicing portions of 208 potential NDD risk genes in over 11,730 ASD, ID, and DD cases. smMIPs provide a highly sensitive, specific, and inexpensive approach to target sequence the protein-coding portions of a moderate number of candidate genes in a large number of patients. Samples were collected as part of an international consortium termed the ASID (Autism Spectrum/Intellectual Disability) network that involved 15 centers across seven countries and four continents. The collection has the advantage over many others in that subsequent phenotypic follow-up is possible for a large fraction of the patients.

RESULTS

Mutation discovery

We selected 208 candidate NDD (ASD, ID and DD) disease-risk genes based on published sequencing studies^{11–17} (Supplementary Tables 1–3) using denovo-db (<http://denovo-db.gs.washington.edu>)¹⁸. Genes were selected and ranked based on the number of published DN recurrences, overlap with a CNV morbidity map¹⁹, pathway connectivity²⁰, and absence of DN variants in 1,909 published unaffected sibling control exomes^{12,13}. We designed 12,016 smMIPs distributed across four smMIP pools to cover all annotated RefSeq coding exons as well as five base pairs of flanking intronic sequence (Supplementary Tables 4–7; Methods). We targeted these genes for sequencing in 15 large cohorts of patients (some including unaffected siblings) with a primary ascertainment diagnosis of ASD, ID, or DD where exome sequencing had not previously been performed (Supplementary Tables 8 and 9). The set includes 6,342 patients with a primary diagnosis of ASD and 7,065 patients diagnosed with ID/DD, representing a large international collaboration between research and clinical investigators from the United States, Belgium, The Netherlands, Sweden, Italy, China, and Australia (Fig. 1).

After quality control (QC; Methods; Supplementary Table 10; Supplementary Fig. 1–4), we identified 61,315 QC-passing variants, excluding common dbSNP variants (<http://www.ncbi.nlm.nih.gov/SNP/>; Methods; Supplementary Table 10). 2,185 were private (i.e., found in only one family in the study; Supplementary Tables 10 and 11) and potentially deleterious (e.g., nonsense, stop-gain, start-loss, frameshift, or disruptive splicing mutations) or missense events with a combined annotation dependent depletion (CADD) score > 30

(MIS30). The number of private, high-impact events identified in probands was significantly greater than in unaffected siblings in the study (false discovery rate (FDR) corrected $p = 1.44 \times 10^{-9}$; Fisher's exact test; Supplementary Fig. 5a,b), as expected^{9,11}. This signal was driven primarily by LGD (corrected $p = 9.20 \times 10^{-15}$) and not MIS30 (corrected $p = 0.83$) events. We validated 1,125 variants, including all private LGD events as well as 25% of the private MIS30 events by Sanger sequencing (validation rate > 97%; Supplementary Table 11).

Genes with an excess of severe *de novo* mutation

We assessed inheritance for 286 of the private variants, 35% of which were determined to be sporadic mutations (Supplementary Tables 12 and 13; Supplementary Fig. 5c). The set represents 91 private DN mutations—82 LGD and 9 MIS30—among cases and 9 DN mutations—3 LGD and 6 MIS30—among unaffected siblings and includes 35 recently reported events^{11,12,21} (Supplementary Table 12; Supplementary Fig. 5d). Allowing for an allele count (AC) ≤ 3 , we identify an additional 32 DN LGD and 15 DN MIS30 events in probands, for a total of 138 DN proband events (114 LGD and 24 MIS30; Supplementary Table 12). Using a probabilistic model derived from human–chimpanzee divergence and an expected rate of 1.5 DN mutations per exome^{9,22}, we calculate the overall probability of detecting 114 or more DN LGD and 24 DN MIS30 variants in our panel of 208 genes, as $p = 1.6 \times 10^{-22}$ (binomial test) with an odds ratio (OR) of 2.62 (95% CI 2.2–3.09). Combining these results (Supplementary Table 12) with published exome datasets (Supplementary Tables 1 and 2), we identify a total of 393 DN LGD and 98 DN MIS30 events in 208 screened genes, increasing the significance ($p = 1.28 \times 10^{-218}$; OR = 6.46; [95% CI 5.89–7.06]). Excluding known high-risk NDD genes (Supplementary Table 3), we recalculated the probability of identifying 136 or more DN LGD and 13 DN MIS30 variants among the 84 unknown genes (Supplementary Table 3) where at least one DN LGD mutation has been identified. The frequency of DN mutations is significantly enriched in probands ($p = 1.32 \times 10^{-55}$, OR = 5.12 [95% CI 4.33–6.01]) suggesting that many of these remaining genes contribute to NDD pathology.

Combining both smMIPs and exome sequence data, we identify 68 genes that reach DN significance for LGD mutations and 23 genes for MIS30 mutations at the level of the individual gene ($q < 0.1$ by binomial test and more than one LGD or MIS30 event in probands; Table 1; Fig. 2a–c; Supplementary Fig. 6; Supplementary Table 14). Thirteen genes were significant for both DN LGD and MIS30 genes; thus, 78 unique genes show an excess of DN mutations in patients (Table 1). Ten (13%) of these genes are unique to the MIS30 category for probands: *TANC2*, *TRIO*, *COL4A3BP*, *TBL1XR1*, *PPP2R5D*, *DLGAP1*, *SRGAP3*, *PTPN11*, *ADCY5*, and *ITPR1* (Table 1; Supplementary Table 15). Thirty-nine of the DN LGD and seven of the DN MIS30 significant genes had been previously linked to NDDs in the literature (Supplementary Table 15; Table 1). Of the 78 DN significant genes, 32 have not been previously described as associated with NDD phenotypes in the literature. The most significant of these genes are *TRIP12*, *KMT5B*, and *ASH1L* (Fig. 3), which were significant for both DN LGD and MIS30 mutations, and *NAA15* and *DSCAM*¹¹ for DN LGD mutations only (corrected $p < 1 \times 10^{-6}$). The most frequently DN mutated genes in this study were *SCN2A*, *ADNP*, *CHD8*, *DYRK1A*, and

POGZ (Supplementary Table 13). DN mutations in *NAA15* were also seen as frequently as *DYRK1A* and *POGZ* (Supplementary Table 13). No genes reach DN LGD significance in unaffected sibling controls; although one gene, *TRRAP*, reaches DN MIS30 significance among the controls. While it is possible that DN mutation of this gene is protective, it is more likely that *TRRAP* represents a false positive possibly due to an elevated mutation rate compared to expectations based on our statistical model.

Inherited mutations and burden

The majority of validated LGD and MIS30 private variants were inherited (65%) either from mother (33.2%) or father (31.8%) (Supplementary Table 13; Supplementary Fig. 5e). Combined with additional ultra-rare ($AC \leq 3$) inherited events (Supplementary Table 16) and published private inherited counts from exome sequencing of the Simons Simplex Collection (SSC)¹³ (Supplementary Table 17), we observe a nominally significant maternal transmission bias for LGD (but not MIS30) events ($p = 0.037$, binomial test where sex chromosome events were excluded). Although currently underpowered at the single-gene level to detect specific genes, several showed an elevated number of maternal transmissions ($\geq 3:1$ ratio; i.e., *AHNAK*, *DSCAM*, *NRXN1*, *NISCH*, *UIMC1*, *PLXNB1*, *PROX2*, *CHD1*, *TNRC18*, *PTK7*, and *MOV10*, Supplementary Fig. 7).

We also estimated the burden of private LGD and MIS30 variants at the single-gene level regardless of inheritance status by comparison with controls from the ExAC database where neuropsychiatric cases had been excluded ($n = 45,376$; <http://exac.broadinstitute.org/>; Supplementary Table 18). Separate simulations of LGD and MIS30 events identify 30 and 13 genes with a significant LGD burden and MIS30 burden, respectively (1×10^6 simulations with Benjamini-Hochberg correction; Table 2; Fig. 2d,e). Four genes—*FOXP1*, *GRIN2B*, *SCN2A*, and *SETD5*—were significant for both LGD and MIS30 burden and are well-established NDD genes. Interestingly, 18 genes—8 LGD and 10 MIS30—had a significant burden of private disruptive mutations in this study but did not reach DN significance likely due to our inability to test inheritance for all events. Although DN mutations in some of these genes have already been implicated in other NDD studies (e.g., *FOXP1*²³, *TRIO*²⁴, *SCN1A*²⁵, *SIN3A*²⁶, and *IQSEC2*²⁷), for others—*CTNND2*, *NAV2*, and *UNC80*—many of the severe mutations in pedigrees are inherited (Supplementary Tables 11 and 16). Given their involvement in neuronal function, axonal projection, dendrite spine formation and oligodendrocyte differentiation^{28–31}, these genes likely begin to define a class of inherited high-impact risk factors.

Autism versus intellectual disability and developmental delay

To determine whether individual genes show a bias for clinical phenotype, we performed a separate burden analysis by primary ascertainment diagnosis (i.e., ASD or ID (including DD diagnoses per DSM-5 criteria)) combined with data from previous NDD studies (Supplementary Tables 2, 11, and 17)¹³. We identify 25 genes that show a bias for primary diagnosis (two one-tailed binomial tests, $p < 0.025$ for either ASD or ID/DD cases) considering both LGD and MIS30 (Fig. 4a). Eight genes have an ASD bias—*CHD2*, *CTTNBP2*, *CHD8*, *LAMC3*, *DIP2A*, *RELN*, *UNC80*, and *IQGAP3*. Of these, only *CHD8*, *CHD2*, and *DIP2A* have been previously implicated as high-risk ASD loci³². Of the 17

ID/DD biased genes, *NAA15*, *ZMYM2*, *PHIP*, and *STAG1* have not been previously linked to these phenotypes. We further separated the LGD and MIS30 events and identified additional significant genes for each mutation type, notably a bias for *CDH10* LGD and *NEMF* MIS30 mutations in ASD (Supplementary Fig. 8a) and *SCN1A* LGD and *NRXN1* MIS30 mutations in ID/DD (Supplementary Fig. 8b). Most genes, however, are mutated in both conditions further highlighting the substantial genetic overlap between these comorbid conditions.

Phenotypic assessment of new risk genes

We recontacted individuals with mutations in *NAA15*, *KMT5B*, and *ASH1L* for further follow-up. We identified 12 LGD and one MIS30 private (Supplementary Table 11) variants in *NAA15* through our smMIP screening (Fig. 3a) and determined that four LGD mutations were sporadic while two LGD variants, including a C-terminal mutation, were inherited (Supplementary Table 11). *NAA15* shows a burden of LGD events in cases (Table 2) as well as an excess of DN LGD variants (Table 1). The gene *NAA15* encodes a protein that is a component of the NatA N-acetyltransferase complex, which includes NAA10—a protein associated with Ogden syndrome as well as non-syndromic DD³³ and is thought to tether the complex to the ribosome for posttranslational modification of proteins as they exit the ribosome³⁴. In order to identify additional patients for clinical recontact, we relaxed our variant filter to allow for ultra-rare ($AC \leq 3$) alleles. In total, we were able to collect clinical information for ten probands with private and three probands with ultra-rare variants in *NAA15* (Supplementary Table 19). Patients in our study with *NAA15* LGD and MIS30 mutations share phenotypic features, including ID (10/11 patients [91%]), speech delay (5/6 patients [83%]), ASD diagnosis (formal diagnosis in 5/8 patients [63%] with ASD-like traits observed in two additional patients), and nonspecific growth abnormalities (e.g., microcephaly, macrocephaly, and hypertelorism) (Supplementary Table 19). Given the incidence of DD (5.12%) in the general population^{35,36}, we estimate the penetrance of LGD *NAA15* mutations to be significant at 35.3% (95% CI 15.7%–63.6%).

Both genes—*KMT5B* and *ASH1L*—encode histone-lysine N-methyltransferase proteins thought to be important in chromatin modification, occupancy and gene regulation. Although the role of these genes in NDDs has not been established, a paralog of *ASH1L*—*SETBP1*—has been shown to be mutated in NDD cases and associated with ID and loss of expressive language¹⁹. We identified two DN LGD and two DN MIS30 mutations in *KMT5B* in this study (Supplementary Table 12) in addition to three DN LGD and one DN MIS30 published variants^{12,14} (Supplementary Table 2; Fig. 3b). We were able to collect clinical information from three probands with private variants and four probands with ultra-rare variants in *KMT5B* (Supplementary Table 20). Patients with disruptive variation in *KMT5B* shared features such as ID/DD (7/7 patients [100%]), ASD diagnosis (5/6 patients [83%]), language delay (3/4 patients [75%]), motor delay (3/5 patients [60%]), and febrile seizures (3/5 patients [60%]). Attention deficits were also observed in three of these patients (Supplementary Table 20). For *ASH1L*, we identified two DN LGD and two DN MIS30 mutations in addition to the three DN LGD previously published mutations^{13,14}. We identified many additional LGD and MIS30 variants in *ASH1L* where parental DNA was not available (Fig. 3c) and found that mutations cluster around the known annotated protein

domains. We were able to obtain clinical information for two probands carrying private and three probands carrying ultra-rare *ASHIL* variants. Individuals with *ASHIL* disruptive variation in this study had ID (5/5 patients [100%]), ASD (2/3 patients [67%]), and evidence of seizures (2/3 patients [67%]) (Supplementary Table 21).

Phenotypic comparisons and a high-functioning ASD network

We selected patients with DN LGD mutations in 25 of our top-ranked genes in an effort to more broadly compare phenotypic features. Of the recontacted individuals, 70% (88/125) agreed to participate in a more comprehensive phenotypic evaluation (Supplementary Methods). To increase our power to detect differences between patients grouped by gene, 215 case reports from the published literature were combined with the findings collected as part of our recontact study. We assessed the general severity of each NDD using a modified de Vries scale (Supplementary Table 22) and summarized phenotypic features collected during follow-up (Table 3: including rates of ASD, ID, seizures, macro/microcephaly, and congenital abnormalities as well as mean IQ measures and ASD severity).

Several specific and global patterns emerged from this combined dataset, in particular, an inverse relationship between ASD and ID diagnoses by gene (Pearson's $R = -0.81$, $p = 9.84 \times 10^{-7}$; Fig. 4b). We partitioned patients into two categories: those most strongly associated with ASD (diagnostic rate $> 95\%$) versus those more strongly associated with DD. Patients with mutations in ASD genes show significantly lower rates of seizures ($p = 1.20 \times 10^{-4}$), congenital abnormalities ($p = 1.88 \times 10^{-2}$), and microcephaly ($p = 1.79 \times 10^{-7}$), but higher rates of macrocephaly ($p = 5.25 \times 10^{-3}$) compared to comorbid ASD and ID genes and strong ID genes (two-tailed Fisher's exact test; Fig. 4c). In addition, the ASD-dominated genes show a significant difference with respect to gender. ASD genes are more likely ($p = 1.65 \times 10^{-4}$) to affect males with an overall ratio of 4:1 when compared to other genes (1.2:1 male to female ratio). Although the number of individual patients per gene is still low, it is interesting that several genes show an exclusive male bias (*KDM6B*, *DSCAM*, *WDFY3*, *CHD1*, and *WDR33*; Fig. 4c; Table 3). Pathway analysis of these 11 ASD genes indicates a functional enrichment for chromatin remodeling (corrected $p = 4.72 \times 10^{-3}$; Enrichr tool (<http://amp.pharm.mssm.edu/Enrichr/>))³⁷ implicating a functional network associated specifically with ASD individuals without ID.

To identify additional genes that may be associated specifically with high-functioning ASD, we revisited the deep phenotyping data collected as part of the SSC and applied the MAGI network-building tool, which compares the spectrum of DN mutations in probands and unaffected siblings to identify co-expression and protein-interaction networks enriched in patients^{12,13,20}. We specifically selected patients with a full-scale IQ (FSIQ) > 100 ($n = 668$ SSC probands; male bias 9:1) to construct a protein-interaction network based on genes with DN variants in this subset (Supplementary Methods). One statistically significant model emerged ($p < 0.01$, simulation test; Fig. 4d), including 40 genes and DN mutations in 31 individuals with FSIQ > 100 . Although mostly comprised of DN missense mutations, the network shows that DN LGD mutations in *FBXW11*, *CHD1*, *CHD8*, *DOT1L*, *HDAC3*, *YTHDC1*, and *KLHDC10* may be important in this patient subset. Both *CHD1* and *CHD8* individuals were included in our large-scale patient recontact and showed high specificity for

ASD diagnosis (Table 3). A pathway analysis for this specific set of genes implicates, once again, chromatin remodeling ($p = 0.0003$ adjusted p -value) as well as mRNA splicing ($p = 0.00026$) and Wnt signaling ($p = 0.03$) as potentially important for ASD without ID.

Functional characterization of candidate genes in *Drosophila*

In order to provide additional functional evidence especially with respect to nervous system function and behavior, we performed a pilot study investigating 21 genes in *Drosophila melanogaster* (Supplementary Table 23). For 11 of these genes, DN LGD mutations are significantly enriched in NDD patients. For the other ten genes, there are indications that they may be associated with ASD, such as a higher mutation rate in ASD cohorts or a central position in ASD gene interaction networks²⁰. Others, such as *NCKAPI* and *WDFY3*, are at the cusp of statistical significance. We used the UAS-Gal4 system and inducible RNA interference (RNAi) lines to specifically knockdown these genes in *Drosophila* neurons. Whenever their locomotor function and overall vigor allowed (Supplementary Table 23), we subjected these knockdown flies to an ASD- and ID-relevant behavioral assay measuring light-off jump habituation, which has been shown to be affected in a number of ASD- or ID-related *Drosophila* models^{38–43}. In this assay, flies suppress their startle (jump) response to a repeated nonthreatening stimulus (light-off) as a result of experience. Their response thus gradually wanes (Fig. 5a,b). As the most fundamental evolutionarily conserved form of learning, habituation is thought to represent a prerequisite for higher cognitive functions⁴⁴. Beyond that, a number of studies showed defective habituation of neural activity or behavior in ASD^{45–48}, and it has been proposed that disturbed habituation mechanisms could substantially contribute to defective filtering and other ASD features^{49,50}.

We first examined genes that showed a significant excess of DN LGD mutations—*NAA15*, *KMT5B*, *ASHIL*, and *TCF4*—and where human phenotypic data strongly support a role in NDDs. For the *Nat1* (ortholog of *NAA15*, VDRC #110689) knockdown, we observe erect wing, impaired locomotor activity, and adult early lethality (within 1–2 days after eclosion). Upon knockdown of *Nat1* using a second presumably weaker RNAi line (VDRC #17571), flies exhibit normal morphology and locomotion; however, when challenged in the light-off jump paradigm, their initial response is impaired (19% frequency of initial jumping), precluding proper assessment of habituation (Supplementary Table 23). These results support *Nat1*'s crucial role in nervous system development. *Ash1* (ortholog of *ASHIL*) neuronal knockdown flies also showed reduced fitness, and, like *Nat1* flies, could not be scored in the habituation paradigm. *Hmt4-20* (ortholog of *KMT5B*) and *da* (ortholog of *TCF4*) flies, in contrast, were overall healthy but showed specific and significant habituation deficits (Fig. 5a,c), suggesting that both genes play important roles in the molecular machinery that regulates habituation learning.

We observed habituation defects following knockdown of fly homologs for several other significant DN genes, including *SYNGAPI*, *GRIN2B*, and *SRCAP* (Fig. 5c, Supplementary Table 23). In addition, *dom* (*SRCAP*) and *da* (*TCF4*) flies showed significant morphological abnormalities at the neuromuscular junction (NMJ), a well-studied synaptic model system (Supplementary Fig. 9). *NCKAPI*, *WDFY3*, and *GIGYF2* are among the tested genes with

borderline significance based on our human genetic data. Significant habituation defects were observed for *hem* (ortholog of *NCKAPI*), *bchs* (ortholog of *WDFY3*), and *CG11148* (ortholog of *GIGYF2*) knockdown flies (Fig. 5c; Supplementary Table 23). Due to the paucity of patients, little is known regarding the clinical phenotypes associated with loss-of-function mutations of these genes; however, these functional studies suggest an important role in neuronal and cognitive function.

DISCUSSION

Targeted sequencing of candidate genes in a large NDD cohort has identified three overlapping categories of high-risk genes. First, we identify 68 genes that now reach DN LGD mutation significance, 39 of which have previously been described. Due to limited availability of parental samples, this estimate is likely conservative. Second, we highlight 24 genes with a significant excess of DN missense mutations in NDD patients; 63% (15/24) overlap genes with DN LGD significance (e.g., *SCN2A*, *STXBPI*, *CHD2*, and *CASK*) while others are significant based only on an excess of DN MIS30 mutations (e.g., *COL4A3BP*, *TRIO*, *TBL1XR1*, and *PPP2R5D*; Table 1), similar to the Noonan-syndrome gene (*PTPN11*)⁵¹. Finally, 39 genes reach statistical significance based on a case-control burden testing (Table 2). Of interest are the 13 genes without DN mutation significance (*SMARCC2*, *CTNND2*, *SIN3A*, *SCN1A*, *NFIA*, *CDKL5*, *DNAJC6*, *IQSEC2*, *IQGAP3*, *ADGRL2*, *ERBIN*, *NAV2*, and *AGPA2*; Table 2) suggesting potential inherited risk factors^{13,31,52}. In total, 44% (91/208) of our candidate genes reach locus-specific significance for disruptive mutations in 5.7% of patients, closely matching empirical expectations¹². However, mutation of these genes may not be necessary and sufficient to result in disease. We note, for example, nine families (Supplementary Fig. 10) with disruptive mutations in two or more of the candidate genes.

Three genes without previous phenotype information reach a high level of DN significance (*NAA15*, *KMT5B*, and *ASH1L*). *NAA15* was originally identified as an *N*-methyl-D-aspartate (NMDA) glutamate receptor-regulated gene through screens of *NMDAR1* knockout mice⁵³. Knockdown of *Naa15* in *Drosophila* neurons caused severe locomotor defects and lethality. Missense mutations in the *NAA15* interacting gene *NAA10* are known to cause Ogden syndrome, an X-linked disorder of infancy that can result in severe DD, craniofacial anomalies, hypotonia, cardiac arrhythmias, and in some cases death⁵⁴. This is consistent with the DD observed in our patients and the fact that DN LGD mutations have been identified in congenital heart disease patients with NDDs⁵⁵. *KMT5B* and *ASH1L* highlight the importance of histone methyltransferases, like *DNMT3* and *EHMT*⁵⁶, in ID and NDD. Mouse studies have shown that Ash11 protein represses nrxn1 α protein in neurons—a known presynaptic adhesion molecule required for synaptic formation⁵⁷; mutations in *NRXN1* have been associated with ASD⁵⁸. Even less is known about the role the protein encoded by *KMT5B* plays in the developing brain. However, studies suggest that the H4K20me3 mark established by the *KMT5B* protein may be involved in cell cycle regulation in baboon neural stem progenitor cells⁵⁹. Our own analyses in *Drosophila* support a role for *NAA15* and *ASH1L* in neuronal development and for *KMT5B* and *TCF4* in habituation learning (Supplementary Table 23) consistent with patient phenotypes (Supplementary Tables 18–20).

We designed the study such that approximately half of the patients were ascertained based on a primary diagnosis of ASD while the other half were diagnosed initially as ID/DD in an effort to test the diagnostic specificity of particular genes. While most genes are clearly risk factors for NDD broadly⁴, secondary analyses of both the genetic burden and subsequent patient follow-up for 25 genes in 303 patients did highlight genes with a statistical bias toward ASD versus ID/DD diagnosis (Table 3; Fig. 4c). We find that patients with mutations in genes enriched for ASD show significantly lower rates of seizures, congenital abnormalities, and microcephaly, but higher rates of macrocephaly compared to comorbid ASD and ID genes and strong ID genes (Fig. 4c). The latter is interesting in light of the observation of increased brain size and/or weight at early ages in subtypes of ASD when compared to ID or typical toddlers^{60–63}. While the number of exome-sequenced patients with a DN mutation are few (4.6% or 31/668 patients), the data highlight a co-expression and protein-interaction network statistically enriched in high-functioning autism patients (FSIQ > 100) when compared to unaffected siblings. This network is biased for DN missense compared to LGD mutations (2:1) indicating that less severe mutations may be playing a role in ASD without ID. The network highlights both mRNA splicing as well as genes important in chromatin remodeling. The latter implicate early developmental programs that regulate cell proliferation, neural patterning and differentiation, axonal guidance consistent with cellular ASD models^{64–66}, and ASD postmortem^{63,67,68}, genomic^{69,70} and developmental imaging^{60–62} studies.

ONLINE METHODS

Patient samples

Whole-blood or cell line DNA from patients with ASD, ID, or DD diagnosis were collected from 15 international clinical and research cohorts (Fig. 1). Only DNA samples from The Autism Simplex Collection (TASC) and Autism Genetic Resource Exchange (AGRE) cohorts were derived from cell lines. Clinical workup, including diagnostic evaluation, medical examination, and neuropsychological assessment, was made available for many patients upon request, specifically for patients with mutations in *NAA15*, *KMT5B*, and *ASH1L* (case reports in Supplementary Data). Best estimate clinical DSM-5¹ diagnoses were made by experienced, licensed clinicians using all available information collected during the evaluation. For a description, the number of individuals represented, and the primary ascertainment criteria for each cohort in this study, refer to Supplementary Table 8. In addition, 2,867 unaffected sibling control individuals were collected for genetic and phenotypic comparison (Supplementary Table 9). All experiments carried out on these individuals were in accordance with the ethical standards of the responsible committee on human experimentation (institutional and national), and proper informed consent was obtained for sequencing, recontact for inheritance testing, and phenotypic workup. All sequencing of patient samples was performed at the University of Washington, Seattle, WA, USA.

Detailed descriptions of clinical cohorts

Autism Clinical and Genetic Resources in China (ACGC)—This cohort has been described previously²¹.

Autism Genetic Resource Exchange (AGRE)—This cohort has been described previously⁸⁷.

Leuven—The Leuven cohort consists of patients with ASD as diagnosed by the multidisciplinary team in the Expert Centre for Autism Leuven according to DSM-IV-TR (American Psychiatric Association, 2000) criteria. All patients have been examined by a clinical geneticist. Patients with known monogenic conditions have been excluded after a routine genetics workup.

Melbourne & Murdoch—All participants had a DSM-IV or DSM-5 diagnosis of ASD. Diagnoses were community-based performed by a multidisciplinary team (pediatrician, psychologist, and speech pathologist). Diagnoses were confirmed for research purposes through ascertainment of previous ASD and cognitive assessments and a telephone interview with the parents. Information about the pregnancy and birth, developmental milestones, comorbidities, medications, and general health was collected during the interview and from medical records. Current ASD symptomatology was measured via the Social Responsiveness Scale (SRS) or Social Responsiveness Scale – 2nd edition (SRS-2). Pedigrees were obtained for each family detailing the family’s history of medical conditions, mental health disorders, intellectual impairment, ASD diagnoses and ASD traits. DNA was collected from blood or saliva from probands and their parents. Most probands underwent molecular karyotyping for CNVs and single-nucleotide polymorphisms and fragile X DNA testing; older participants had routine karyotyping.

The Autism Simplex Collection (TASC)—This cohort has been described previously⁸⁸.

Adelaide—Individuals with intellectual disability or developmental delay were recruited who were referred but negative for molecular testing for fragile X and large CNVs by array comparative genomic hybridization (CGH). The vast majority were also singletons and recently clinically diagnosed/ascertained patients for recontact purposes.

Leiden—The cohort consists of patients with developmental delay with or without autistic features. Clinical microarrays to detect CNVs were run on all index patients, and identification of a likely causal CNV was an exclusion criterion. No formal DSM criteria were used in the diagnosis. All patients were seen by experienced clinical geneticists and if indicated specific gene tests were requested. Parents of the patients gave verbal consent for inclusion in this study.

Stockholm—Array CGH was performed for all cases using the Agilent platform with a 180k genome-wide design. The cases were referred for genetic investigation due to a diagnosis of ID/ASD but did not use the DSM-5 guidelines systematically.

Candidate gene selection

Candidate genes with DN mutations were identified from whole-exome and targeted sequencing studies of ASD, ID, and DD based on previously published studies and included 4,874 probands with ASD^{9,11–14}, 151 probands with ID^{15,16}, and 1,133 probands with DD¹⁷ (Supplementary Table 1). Genes were ranked based on the following criteria: (1) presence of

two or more LGD mutations, (2) presence of multiple missense mutations and at least one LGD mutation, (3) presence of at least one LGD mutation overlapping a region of interest in our published DD CNV morbidity map¹⁹, and (4) presence of at least one LGD mutation with network connectivity to either chromatin remodeling/transcription or long-term potentiation as described previously²⁰. Genes with expression in the brain (based on the BrainSpan Atlas of the Developing Human Brain [<http://www.brainspan.org/>] and GTEx [<http://www.gtexportal.org/>] databases⁸⁹) were prioritized. We eliminated genes associated with likely unrelated disorders in OMIM (<http://www.omim.org/>) and genes that were deemed highly mutable (determined based on data from 6,503 control individuals in the NHLBI Exome Sequencing Project [ESP; <http://evs.gs.washington.edu/EVS/>]). Finally, we filtered genes based on the number of DN mutations by whole-exome sequencing among unaffected siblings from the SSC^{11–13}. See Supplementary Table 3 for more details on selection criteria.

smMIP sequencing and variant validation

smMIP sequencing was performed as previously described^{9,10}. We targeted the coding portions of all RefSeq annotated transcripts for these 208 genes as well as five base pairs into each exon-adjacent intron in order to capture variation at splice-donor/acceptor sites resulting in the design of 12,016 smMIPs. smMIPs were split into four pools (Gold, ASD4, ASD5, and ASD6; see Supplementary Tables 4–7 for gene breakdown), and each pool was rebalanced so that poorer performing smMIPs were spiked in at a concentration of 10X or 50X. Approximately 192 samples were barcoded and sequenced per lane of Illumina HiSeq 2000 as previously described¹¹, and data analysis was performed using the MIPgen suite of tools (<http://shendurelab.github.io/MIPGEN/>). Variant calling of smMIP data was performed on each sequencing lane using FreeBayes v0.9.14 with default settings and the hg19 reference. For each of the four pools, all FreeBayes output was combined using GATK. Allele counts per genotype (AC) and the total number of alleles per genotype (AN) counts were recalibrated on the combined variant set using VCFtools. Multi-allelic sites were split into separate entries using vcflib (vcfbreakmulti) and sequencing error repeats and common single-nucleotide polymorphisms (all of dbSNP v129 and variants found in dbSNP v141 at a minor allele frequency ≥ 0.01 in at least one major population with at least two unrelated individuals having the minor allele) were removed. From the individual genotypes with sequencing depth (DP) of greater than 8X and a quality score (QUAL) of greater than 20, a private filter (found in only one family in the study) was applied to each pooled dataset (i.e., ASD4, ASD5, ASD6, or Gold). These variants were annotated using the Ensembl Variant Effect Predictor tool for GRCh37 (http://grch37.ensembl.org/Homo_sapiens/Tools/VEP/) and with CADD scores⁹⁰ (<http://cadd.gs.washington.edu/>; v1.3). All private LGD variants and a portion of MIS30 variants were validated by Sanger sequencing. Specifically, a CADD > 30 was chosen for validation as these events are very rare (<0.1% of all missense events in control genomes⁹⁰) and more likely to be pathogenic²¹. Where available, parents were also Sanger sequenced to determine the inheritance status of these variants. In total, we targeted >16,000 unique samples including 13,475 probands and 2,867 unaffected siblings using each of the four smMIP pools. 1,744 of the DNA samples did not have sufficient DNA for all four pools; gene sets were prioritized based on potential disease significance (Gold>ASD4>ASD5>ASD6; Supplementary Table 10) with 13,475 probands (Gold),

12,260 probands (ASD4&5), and 11,731 probands (ASD6). In addition, we sequenced 2,867 unaffected sibling samples with each of the four pools. To determine the performance of each smMIP pool, 10 plates of unaffected siblings (960 samples) were compared in each pool plotting the frequency of these 960 samples that reached at least 8X sequencing coverage for each individual smMIP in the study (Supplementary Table 3). Each of these data points were plotted by gene within each pool (i.e., Gold, ASD4, ASD5, and ASD6 shown in Supplementary Fig. 1–4, respectively). 165 genes passed all QC metrics (75% of smMIPs by gene reached at least 8X coverage in $\geq 80\%$ of controls), but some exons, due to their size or GC composition, failed to pass these thresholds. For those regions that did not pass QC, we chose to consider variant genotypes identified in samples if they were of high quality (read depth (DP) > 8, phred scaled quality score (QUAL) > 20); however, these variants were not considered for assessments of mutation burden.

Clinical recontact and phenotyping

To systematically compare the effect of particular LGD mutations of targeted genes on phenotype, we recontacted individuals with identified LGD mutations and conducted a comprehensive phenotypic workup assessing function across multiple domains. Per our human subjects approval, we only recontacted individuals that had consented to be approached about future studies during their original assessment. Families were invited to participate in a comprehensive clinical workup that included diagnostic evaluation, medical examination, and neuropsychological assessment (see Supplementary Methods for test battery and procedures). Importantly, all assessments were conducted by examiners naïve to the individual's genetic event, thereby reducing clinician bias in rendering diagnostic dispositions. In order to make comparisons across groups with similar LGD mutations, each participant was scored according to a modified version of the de Vries scale as a proxy for the overall severity of the phenotype^{92–94}. The modified de Vries scale included presence of facial dysmorphisms, congenital abnormalities, postnatal head growth abnormalities, ID/DD, and the number of DSM-5 diagnoses and medical diagnoses conferred, allowing a score ranging from zero to twelve (Supplementary Table 22). Data collected from these patients were combined with published case reports to increase our power to detect enrichments among patients sharing DN LGD mutations in the same gene or pathway. A total of 323 case reports of individuals with DN LGD mutations of interest and relevant data were included. The relevant phenotype data extracted from cases in the published literature were combined with information collected from individuals that were able to complete the in-person comprehensive evaluation. The modified de Vries scale score for individuals with the same disrupted gene were averaged and then rank-ordered to estimate the impact of the gene mutation on phenotype. Only genes with six or more study participants and published case reports were included in the analysis. Patients that were considered had LGD mutations in one of the following genes: *ADNP*, *ARID1B*, *CHD2*, *CHD8*, *CTNNA1*, *DYRK1A*, *FOXP1*, *GRIN2B*, *MED13L*, *POGZ*, *PTEN*, *SCN2A*, *SETBP1*, *STXBP1*, or *TBL1XR1*.

Patient workups

Comprehensive clinical workup included diagnostic evaluation, medical examination, and neuropsychological assessment. Best estimate clinical DSM-5¹ diagnoses were made by experienced, licensed clinicians using all available information collected during the research

evaluation. The battery included autism-specific diagnostic measures, the Autism Diagnostic Observation Schedule⁹⁵ and the Autism Diagnostic Interview – Revised⁹⁶, both administered by research-reliable clinicians. The battery also included assessment of cognitive ability (Differential Ability Scales, DAS⁹⁷), language ability (Peabody Picture Vocabulary Test – 4th Edition, PPVT; Expressive Vocabulary Test-2nd Edition, EVT), adaptive functioning (Vineland Adaptive Behavior Scales-2nd Edition) and motor ability (Movement ABC; Purdue Pegboard), as well as behavioral and psychiatric disorders (Child and Adolescent Symptom Inventory, 5th Edition (CASI-5); Child Behavior Checklist (CBCL), Aberrant Behavior Checklist (ABC)). Medical diagnoses were assessed using the SSC medical history interview⁹⁸ and by physical examination conducted by a developmental pediatrician conducting a standardized medical examination.

Participants undergoing comprehensive phenotypic assessment and published case reports in the literature were scored using an adapted de Vries scale as a proxy for the overall severity of the phenotype^{75,76}. Modifications included the removal of stature and prenatal onset growth retardation, the inclusion of medical and psychiatric diagnoses, revision of weighting of intellectual disability into 3 points, and an increase to a total score of 12. Borderline intellectual disability or general delays were rated with 1 point, mild to moderate intellectual disability scored with 2 points, and severe-profound intellectual disability scored with 3 points. Psychiatric and medical diagnoses were tallied and scored 1 if an individual had one diagnosis in these domains and scored 2 if the child had two or more diagnoses in these domains.

DSM-5 diagnoses included: ASD (299.00), attention-deficit hyperactivity disorders (314.01, 314.00), language disorder (315.39), speech sound disorder (315.39), developmental coordination disorder (315.4), anxiety disorders (309.21, 300.29, 300.01, 300.02, 300.09), behavior disorders (313.81, 312.34, 312.81, 312.9), mood disorders (311.0, 296.99, 300.4), elimination disorders (307.6, 307.7). Intellectual disability (319, 315.8) was not tallied in the DSM-5 diagnosis domain. Medical diagnoses were tallied by system: cardiac, gastrointestinal, genital, neurological, pulmonary, renal, and visual and auditory. In order to not double code diagnoses, microcephaly, macrocephaly and congenital abnormalities were not tallied under the medical diagnoses domain.

Relevant phenotypic data were extracted from published case reports of individuals with DN LGD mutations to increase our power to detect enrichments among patients sharing DN LGD mutations in the same gene. A total of 323 case reports of individuals with DN LGD mutations of interest and relevant data were identified and 215 case reports had sufficient data to incorporate in the de Vries scale. LGD mutations included: *ADNP*^{8,17,99}, *ARID1B*^{17,23,100}, *CHD2*^{17,23,101}, *CHD8*^{6,102}, *CTNNB1*^{15,17,103–105}, *DYRK1A*^{7,17}, *FOXP1*^{17,106,107}, *GRIN2B*^{15,17,23,101,108–111}, *MED13L*^{17,23,112,113}, *POGZ*^{17,38,114,115}, *PTEN*^{101,116,117}, *SCN2A*^{15,17,101,118–122}, *SETBP1*^{17,19,23,123–125}, *STXBPI*^{17,101,126}, and *TBL1XR1*^{17,127}.

Network analysis

We investigated modules significantly disrupted in high-functioning autism samples (full-scale IQ > 100). We applied MAGI²⁰ on all of the samples from the ASD probands in SSC

with FSIQ above 100. This subset of samples covers over 500 total missense DN mutations and 100 LGD mutations. We applied the MAGI tool for module discovery on these variants utilizing protein-interaction networks, gene co-expression networks and severe mutations reported in control population from ESP (<http://evs.gs.washington.edu/EVS/>; n = 6,500 individuals). The protein-interaction network used was a combination of networks from HPRD¹²⁸ and String¹²⁹ databases and the co-expression network was built using BrainSpan Atlas resource. Note that the exact same training networks were used in our previous analysis for autism module discovery²⁰. The parameters were that the pairwise gene co-expression inside modules be, on average, at least 0.415 and the average protein interaction density be 0.085. MAGI found one module of 40 genes significantly enriched in DN mutations (p < 0.01 using 100 random mutation permutation tests).

***Drosophila* knockdown models**

Drosophila orthologs of the genes of interest were determined using Ensembl, Unigene, and flybase databases^{130,131}. Their expression was knocked down using the UAS-Gal4 system¹³² to induce conditional RNAi. The panneuronal promoter line *w1118; 2xGMR-wIR; elav-Gal4, UAS-Dicer-2⁴²* and two independent RNAi constructs per gene were used whenever available (www.vdrc.at)¹³³ that fulfilled stringent specificity criteria (s19 value \geq 0.98)¹³⁴. Strains containing identical genetic background to the RNAi constructs (#60000, #60100) were crossed to the driver line and used as controls. No effects in our assays were seen when crossing the '40DUAS' line¹³⁵ (containing UAS repeats but no functional short hairpin RNA, a potential source for dominant phenotypes due to an integration locus of the VDRC KK library^{135,136}) to our panneuronal Gal4 driver. Flies were cultured according to standard procedures. Experimental randomization was not applicable to the *Drosophila* experiments in this study.

***Drosophila* light-off jump reflex habituation assay**

The *Drosophila* light-off jump habituation assay was performed as previously described¹³⁷. Briefly, flies were reared at 25°C and 70% humidity, in a 12:12h light/dark cycle. For all healthy lines, at least 64 3-to-7-day-old male flies were tested per genotype, in at least two independent experiments. Flies were transferred into individual vials of two 16-unit habituation systems (Aktogen Ltd., Hungary) and, after 5 min adaptation, exposed to 100 light-off pulses (15 ms each) with 1-second inter-pulse interval. Their jump responses were recorded by two sensitive microphones placed in each vial. A carefully chosen threshold was applied to distinguish the jump responses from the background noise. Data from 64 individual flies per genotype were collected (two independent experiments) and analyzed by a custom Labview Software (National Instruments). Genotypes were blinded during the experiments and automatically analyzed. Flies that jumped at least once in the first five trials were evaluated for habituation (pre-established criterion). Initial jumping responses to light-off pulse decreased with number of pulses and flies were considered habituated when they stopped jumping for five consecutive trials (no-jump criterion). Habituation was scored as the number of trials to the no-jump criterion (TTC). The main effect of genotype, corrected for testing day and 16-unit system on TTC values, was determined using linear model regression analysis with R statistical software (v.3.0.0).

***Drosophila* NMJ experiments**

Flies were reared at 28°C, 60% humidity and a 12:12h light/dark cycle. Type 1b NMJs of muscle 4 were analyzed. Wandering 3rd instar larvae were collected, dissected and fixed in 3.7% PFA for 30 min. Preparations were rinsed with PBS and permeabilized with 0.3% Triton X-100 in PBS for 2h at room temperature. Discs large protein (Dlg1) was visualized using primary antibody anti-Dlg1 (1:25) (Dlg1-4D6, Developmental Studies Hybridoma Bank) conjugated with the Zenon Alexa Fluor 568 Mouse IgG1 labelling kit (Invitrogen), according to the manufacturer's protocol. The preparations were incubated for 1.5h at room temperature, extensively washed and mounted in ProLong Gold Antifade Mountant (Thermo Fisher Scientific). Genotypes were blinded during the experiments and automatically analyzed. Based on previous experience³⁸⁻⁴⁰ fluorescence images were acquired per genotype using an automated Leica DMI6000B high-content microscope. Morphometric analysis was performed in FIJI¹³⁸ using the *Drosophila* NMJ Morphometrics macro¹³⁹. Resulting images were visually inspected for accurate image segmentation. Inaccurately segmented parameters were excluded as previously described¹³⁹. NMJ boutons number in *hmt4-20* knockdown flies was manually assessed, blinded to genotype, by two independent researchers and averaged to obtain the final counts. Statistical analysis was performed using GraphPad PRISM. Area, perimeter, length, longest branch length, and boutons were analyzed by Student's t-test. Branches, branching points, and islands were analysed by Mann-Whitney U test.

Statistical analyses

To calculate the significance and penetrance of LGD and MIS30 mutations in ASD/ID, we compared our smMIP data to two control datasets: the first included the 2,867 unaffected sibling controls that were sequenced through the same smMIP pipeline (see above), and the second included mutation data from the ExAC database⁹¹ where neuropsychiatric cases were removed (ExAC v0.3), representing 45,376 samples. The .vcf file for these 45,376 ExAC samples was annotated using VEP and CADD (as described above). The ExAC dataset was filtered by the same pipeline as the smMIP data (see above) including only "PASS" variants. Private variants were filtered as an AC = 1 for burden statistics. In order to compare the ExAC control counts to the smMIP data, only LGD and MIS30 events were considered. LGD and MIS30 counts by gene for ExAC can be found in Supplementary Table 18. To calculate the significance of private LGD or MIS30 mutation burden in our smMIP dataset compared to unaffected (ExAC) controls, we performed a simulation by shuffling the labels of private case and control observations 1x10⁶ times and calculated the probability of observing at least the number of LGD or MIS30 events seen among our cases. These p-values were corrected (Benjamini-Hochberg) for the number of genes in the study (n = 208). Penetrance and its confidence bounds were calculated using the model described previously³⁶:

$$P(D|G) = \frac{P(G|D) P(D)}{P(G|D) P(D) + P(G|\bar{D}) P(\bar{D})}$$

where D = disease, G = genotype (the presence of the specific type of event in the gene), and \bar{D} = absence of disease. The general population incidence of ID/DD in our cohort was assumed to match that described in Rosenfeld et al.^{35,36} ($P(D) = 5.12\%$), as our cohort composition has a similar representation of youth onset diseases with an important genetic component with broad exclusion of chromosomal disorders. DN significance was calculated as previously described⁹ using a statistical framework that considers the length of the gene and divergence between chimpanzee and human. In order to calculate DN significance for MIS30 variants, we modified the model to separately enumerate prior probabilities for CADD < 30 and CADD \geq 30 missense sites using CADD v1.3.

To compare clinical phenotypes, a Pearson's correlation coefficient and p value were used to compare overall ASD versus ID diagnosis by genic event. Phenotypic rates were compared between individuals carrying variants in ASD versus DD genes using a two-tailed Fisher's exact test.

A linear model regression analysis was performed using 64 flies per genotype collected through two independent experiments for the habituation data calculations. For the NMJ experiments, area, perimeter, length, longest branch length, and boutons were analysed by two-tailed Student's t-test (degrees of freedom for *SRCAP* (*dom*) experiments: Area = 60, Length = 65, Boutons = 73, Perimeter = 60; degrees of freedom for *TCF4* (*da*) experiments: Area = 63, Length = 68, Branches = 68, Branching = 68). Branches, branching points, and islands were analysed by Mann-Whitney U test.

Supplementary Material

Refer to Web version on PubMed Central for supplementary material.

Authors

Holly A. F. Stessman^{1,Ψ,α}, Bo Xiong^{1,2,Ψ}, Bradley P. Coe^{1,β}, Tianyun Wang^{3,β}, Kendra Hoekzema¹, Michaela Fenckova^{4,5}, Malin Kvarnung^{6,7}, Jennifer Gerds⁸, Sandy Trinh⁸, Nele Cosemans⁹, Laura Vives¹, Janice Lin¹, Tychele N. Turner¹, Gijs Santen¹⁰, Claudia Ruivenkamp¹⁰, Marjolein Kriek¹⁰, Arie van Haeringen¹⁰, Emmelien Aten¹⁰, Kathryn Friend^{11,12}, Jan Liebelt¹³, Christopher Barnett¹³, Eric Haan^{11,13}, Marie Shaw¹¹, Jozef Gecz^{11,14}, Britt-Marie Anderlid^{6,7}, Ann Nordgren^{6,7}, Anna Lindstrand^{6,7}, Charles Schwartz¹⁵, R. Frank Kooy¹⁶, Geert Vandeweyer¹⁶, Celine Helmsmoortel¹⁶, Corrado Romano¹⁷, Antonino Alberti¹⁷, Mirella Vinci¹⁷, Emanuela Avola¹⁷, Stefania Giusto¹⁸, Eric Courchesne¹⁹, Tiziano Pramparo¹⁹, Karen Pierce¹⁹, Srinivasa Nalabolu¹⁹, David Amaral²⁰, Ingrid E. Scheffer^{21,22,23}, Martin B. Delatycki^{21,24,25}, Paul J. Lockhart^{21,25}, Fereydoun Hormozdiari²⁶, Benjamin Harich^{4,5}, Anna Castells-Nobau^{4,5}, Kun Xia³, Hilde Peeters⁹, Magnus Nordenskjöld^{6,7}, Annette Schenck^{4,5}, Raphael A. Bernier⁸, and Evan E. Eichler^{1,27}

Affiliations

¹Department of Genome Sciences, University of Washington, Seattle, WA, USA

²Department of forensic medicine and Institute of Brain Research, Tongji Medical

College, Huazhong University of Science and Technology, Wuhan, Hubei, China
³The State Key Laboratory of Medical Genetics, School of Life Sciences, Central South University, Changsha, Hunan, China ⁴Department of Human Genetics, Radboud university medical center, Nijmegen, The Netherlands ⁵Donders Institute for Brain, Cognition and Behaviour, Radboud university medical center, Nijmegen, The Netherlands ⁶Department of Molecular Medicine and Surgery, Center for Molecular Medicine, Karolinska Institutet, Stockholm, Sweden ⁷Department of Clinical Genetics, Karolinska University Hospital, Stockholm, Sweden ⁸Department of Psychiatry and Behavioral Sciences, University of Washington, Seattle, WA, USA ⁹Centre for Human Genetics, KU Leuven and Leuven Autism Research (LAuRes), Leuven, Belgium ¹⁰Department of Clinical Genetics, Leiden University Medical Center (LUMC), Leiden, The Netherlands ¹¹Robinson Research Institute and the University of Adelaide at the Women's and Children's Hospital, North Adelaide, Australia ¹²SA Pathology, Adelaide, Australia ¹³South Australian Clinical Genetics Service, SA Pathology (at Women's and Children's Hospital), Adelaide, Australia, Australia ¹⁴South Australian Health and Medical Research Institute, Adelaide, Australia ¹⁵Center for Molecular Studies, J.C. Self Research Institute of Human Genetics, Greenwood Genetic Center, Greenwood, South Carolina, USA ¹⁶Department of Medical Genetics, University of Antwerp, Antwerp, Belgium ¹⁷Unit of Pediatrics & Medical Genetics ¹⁸Unit of Neurology, IRCCS Associazione Oasi Maria Santissima, Troina, Italy ¹⁹UCSD, Autism Center of Excellence, La Jolla, CA, USA ²⁰MIND Institute and the University of California Davis School of Medicine, Sacramento, CA, USA ²¹Department of Paediatrics, University of Melbourne, Royal Children's Hospital, Melbourne, Victoria, Australia ²²Department of Medicine, University of Melbourne, Austin Health, Melbourne, Australia ²³The Florey Institute of Neuroscience and Mental Health, Parkville, Victoria, Australia ²⁴Victorian Clinical Genetics Services, Parkville, Victoria, Australia ²⁵Bruce Lefroy Centre for Genetic Health Research, Murdoch Children's Research Institute, Parkville, Victoria, Australia ²⁶Department of Biochemistry and Molecular Medicine, University of California at Davis, Davis, CA, USA ²⁷Howard Hughes Medical Institute, Seattle, WA, USA

Acknowledgments

We thank the individuals and their families for participation in this study. We acknowledge the Vienna Drosophila Resource Center and Bloomington Drosophila stock center (NIH P40OD018537). This research was supported, in part, by the following: Simons Foundation Autism Research Initiative (SFARI 303241) and NIH (R01MH101221) to E.E.E., VIDI and TOP grants (917-96-346, 912-12-109) from the Netherlands Organization for Scientific Research and Horizon 2020 Marie Skłodowska-Curie European Training Network (MiND, 643051) to A.S., the NHGRI Interdisciplinary Training in Genome Science Grant (T32HG00035) to H.A.F.S. and T.N.T., Australian NHMRC grants 1091593 and 1041920 and Channel 7 Children's Research Foundation support to J.G., the National Basic Research Program of China (2012CB517900) and the National Natural Science Foundation of China (81330027, 81525007 and 31400919) to K.X., the China Scholarship Council (201406370028) and the Fundamental Research Funds for the Central Universities (2012zzts110) to T.W., the National Health and Medical Research Council of Australia Project Grants (556759) and (1044175) to I.E.S., P.J.L. and M.B.D., Practitioner Fellowship (1006110) to I.E.S., grants from the Jack Brockhoff Foundation and Perpetual Trustees, the Victorian State Government Operational Infrastructure Support and Australian Government NHMRC IRIISS, the Swedish brain foundation, the Swedish Research Council, the Stockholm County Council, grants (KL2TR00099 and 1KL2TR001444) from the University of California, San Diego Clinical and Translational Research Institute to T.P.,

and the Research Fund - Flanders (FWO) to R.F.K. and G.V.D.W. We are grateful to all of the families at the participating Simons Simplex Collection (SSC) sites, as well as the principal investigators (A. Beaudet, R. Bernier, J. Constantino, E. Cook, E. Fombonne, D. Geschwind, R. Goin-Kochel, E. Hanson, D. Grice, A. Klin, D. Ledbetter, C. Lord, C. Martin, D. Martin, R. Maxim, J. Miles, O. Ousley, K. Pelphrey, B. Peterson, J. Piggot, C. Saulnier, M. State, W. Stone, J. Sutcliffe, C. Walsh, Z. Warren, E. Wijsman). We appreciate obtaining access to phenotypic data on SFARI Base. We gratefully acknowledge the resources provided by the Autism Genetic Resource Exchange (AGRE) Consortium and the participating AGRE families. AGRE is a program of Autism Speaks and is supported, in part, by grant 1U24MH081810 from the National Institute of Mental Health to Clara M. Lajonchere (PI). Approved researchers can obtain the SSC population dataset described in this study (<http://sfari.org/resources/simons-simplex-collection>) by applying at <https://base.sfari.org>. We thank N. Brown, K. Pereira, T. Vick, T. Desai, C. Green, A. L. Doebly, and L. Grillo for their valuable contributions as well as T. Brown for assistance in editing this manuscript. H.P. is a Senior Clinical Investigator of The Research Foundation-Flanders (FWO). E.E.E. is an investigator of the Howard Hughes Medical Institute.

Abbreviations

ASD	autism spectrum disorders
CNV	copy number variant
ID	intellectual disability
DD	developmental delay
NDD	neurodevelopmental disorder
DN	<i>de novo</i>
LGD	likely gene-disruptive
smMIP	single-molecule molecular inversion probe
CADD	combined annotation dependent depletion
MIS30	missense mutations with a CADD score > 30
SSC	Simons Simplex Collection
FDR	false discovery rate
NMJ	neuromuscular junction
TTC	trials to no-jump criterion

References

1. Diagnostic and statistical manual of mental disorders. 5. American Psychiatric Association; 2013.
2. Posthuma D, Polderman TJ. What have we learned from recent twin studies about the etiology of neurodevelopmental disorders? *Curr Opin Neurol*. 2013; 26:111–21. [PubMed: 23426380]
3. Torres F, Barbosa M, Maciel P. Recurrent copy number variations as risk factors for neurodevelopmental disorders: critical overview and analysis of clinical implications. *J Med Genet*. 2015
4. Matson JL, Shoemaker M. Intellectual disability and its relationship to autism spectrum disorders. *Res Dev Disabil*. 2009; 30:1107–14. [PubMed: 19604668]
5. Stessman HA, Bernier R, Eichler EE. A genotype-first approach to defining the subtypes of a complex disease. *Cell*. 2014; 156:872–7. [PubMed: 24581488]

6. Bernier R, et al. Disruptive CHD8 Mutations Define a Subtype of Autism Early in Development. *Cell*. 2014; 158:263–76. [PubMed: 24998929]
7. van Bon BW, et al. Disruptive de novo mutations of DYRK1A lead to a syndromic form of autism and ID. *Mol Psychiatry*. 2016; 21:126–32. [PubMed: 25707398]
8. Helsmoortel C, et al. A SWI/SNF-related autism syndrome caused by de novo mutations in ADNP. *Nat Genet*. 2014; 46:380–4. [PubMed: 24531329]
9. O’Roak BJ, et al. Multiplex targeted sequencing identifies recurrently mutated genes in autism spectrum disorders. *Science*. 2012; 338:1619–22. [PubMed: 23160955]
10. Hiatt JB, Pritchard CC, Salipante SJ, O’Roak BJ, Shendure J. Single molecule molecular inversion probes for targeted, high-accuracy detection of low-frequency variation. *Genome Res*. 2013; 23:843–54. [PubMed: 23382536]
11. O’Roak BJ, et al. Recurrent de novo mutations implicate novel genes underlying simplex autism risk. *Nat Commun*. 2014; 5:5595. [PubMed: 25418537]
12. Iossifov I, et al. The contribution of de novo coding mutations to autism spectrum disorder. *Nature*. 2014; 515:216–21. [PubMed: 25363768]
13. Krumm N, et al. Excess of rare, inherited truncating mutations in autism. *Nat Genet*. 2015; 47:582–8. [PubMed: 25961944]
14. De Rubeis S, et al. Synaptic, transcriptional and chromatin genes disrupted in autism. *Nature*. 2014; 515:209–15. [PubMed: 25363760]
15. de Ligt J, et al. Diagnostic exome sequencing in persons with severe intellectual disability. *N Engl J Med*. 2012; 367:1921–9. [PubMed: 23033978]
16. Rauch A, et al. Range of genetic mutations associated with severe non-syndromic sporadic intellectual disability: an exome sequencing study. *Lancet*. 2012; 380:1674–82. [PubMed: 23020937]
17. Deciphering Developmental Disorders, S. Large-scale discovery of novel genetic causes of developmental disorders. *Nature*. 2015; 519:223–8. [PubMed: 25533962]
18. Turner TN, et al. denovo-db: a compendium of human de novo variants. *Nucleic Acids Res*. 2016
19. Coe BP, et al. Refining analyses of copy number variation identifies specific genes associated with developmental delay. *Nat Genet*. 2014; 46:1063–71. [PubMed: 25217958]
20. Hormozdiari F, Penn O, Borenstein E, Eichler EE. The discovery of integrated gene networks for autism and related disorders. *Genome Res*. 2015; 25:142–54. [PubMed: 25378250]
21. Wang T, et al. De novo genic mutations among a Chinese autism spectrum disorder cohort. *Nat Commun*. 2016; 7:13316. [PubMed: 27824329]
22. Turner TN, et al. Genome Sequencing of Autism-Affected Families Reveals Disruption of Putative Noncoding Regulatory DNA. *Am J Hum Genet*. 2016; 98:58–74. [PubMed: 26749308]
23. Hamdan FF, et al. De novo mutations in FOXP1 in cases with intellectual disability, autism, and language impairment. *Am J Hum Genet*. 2010; 87:671–8. [PubMed: 20950788]
24. Ba W, et al. TRIO loss of function is associated with mild intellectual disability and affects dendritic branching and synapse function. *Hum Mol Genet*. 2016; 25:892–902. [PubMed: 26721934]
25. Han S, et al. Autistic-like behaviour in *Scn1a*^{+/-} mice and rescue by enhanced GABA-mediated neurotransmission. *Nature*. 2012; 489:385–90. [PubMed: 22914087]
26. Witteveen JS, et al. Haploinsufficiency of MeCP2-interacting transcriptional co-repressor SIN3A causes mild intellectual disability by affecting the development of cortical integrity. *Nat Genet*. 2016; 48:877–87. [PubMed: 27399968]
27. Shoubridge C, et al. Mutations in the guanine nucleotide exchange factor gene IQSEC2 cause nonsyndromic intellectual disability. *Nat Genet*. 2010; 42:486–8. [PubMed: 20473311]
28. Chan CB, et al. PIKE is essential for oligodendroglia development and CNS myelination. *Proc Natl Acad Sci U S A*. 2014; 111:1993–8. [PubMed: 24449917]
29. McNeill EM, et al. Nav2 hypomorphic mutant mice are ataxic and exhibit abnormalities in cerebellar development. *Dev Biol*. 2011; 353:331–43. [PubMed: 21419114]

30. Stray-Pedersen A, et al. Biallelic Mutations in UNC80 Cause Persistent Hypotonia, Encephalopathy, Growth Retardation, and Severe Intellectual Disability. *Am J Hum Genet.* 2016; 98:202–9. [PubMed: 26708751]
31. Turner TN, et al. Loss of delta-catenin function in severe autism. *Nature.* 2015; 520:51–6. [PubMed: 25807484]
32. Sanders SJ, et al. Insights into Autism Spectrum Disorder Genomic Architecture and Biology from 71 Risk Loci. *Neuron.* 2015; 87:1215–33. [PubMed: 26402605]
33. Rope AF, et al. Using VAAST to identify an X-linked disorder resulting in lethality in male infants due to N-terminal acetyltransferase deficiency. *Am J Hum Genet.* 2011; 89:28–43. [PubMed: 21700266]
34. Liszczak G, et al. Molecular basis for N-terminal acetylation by the heterodimeric NatA complex. *Nat Struct Mol Biol.* 2013; 20:1098–105. [PubMed: 23912279]
35. Baird PA, Anderson TW, Newcombe HB, Lowry RB. Genetic disorders in children and young adults: a population study. *Am J Hum Genet.* 1988; 42:677–93. [PubMed: 3358420]
36. Rosenfeld JA, Coe BP, Eichler EE, Cuckle H, Shaffer LG. Estimates of penetrance for recurrent pathogenic copy-number variations. *Genet Med.* 2013; 15:478–81. [PubMed: 23258348]
37. Chen EY, et al. Enrichr: interactive and collaborative HTML5 gene list enrichment analysis tool. *BMC Bioinformatics.* 2013; 14:128. [PubMed: 23586463]
38. Stessman HA, et al. Disruption of POGZ Is Associated with Intellectual Disability and Autism Spectrum Disorders. *Am J Hum Genet.* 2016; 98:541–52. [PubMed: 26942287]
39. Esmaeli-Nieh S, et al. BOD1 Is Required for Cognitive Function in Humans and Drosophila. *PLoS Genet.* 2016; 12:e1006022. [PubMed: 27166630]
40. Lugtenberg D, et al. De novo loss-of-function mutations in WAC cause a recognizable intellectual disability syndrome and learning deficits in Drosophila. *Eur J Hum Genet.* 2016; 24:1145–53. [PubMed: 26757981]
41. Kleefstra T, et al. Disruption of an EHMT1-associated chromatin-modification module causes intellectual disability. *Am J Hum Genet.* 2012; 91:73–82. [PubMed: 22726846]
42. van Bon BW, et al. CEP89 is required for mitochondrial metabolism and neuronal function in man and fly. *Hum Mol Genet.* 2013; 22:3138–51. [PubMed: 23575228]
43. Willemsen MH, et al. GATAD2B loss-of-function mutations cause a recognisable syndrome with intellectual disability and are associated with learning deficits and synaptic undergrowth in Drosophila. *J Med Genet.* 2013; 50:507–14. [PubMed: 23644463]
44. Schmid S, Wilson DA, Rankin CH. Habituation mechanisms and their importance for cognitive function. *Front Integr Neurosci.* 2014; 8:97. [PubMed: 25620920]
45. Kleinhans NM, et al. Reduced neural habituation in the amygdala and social impairments in autism spectrum disorders. *Am J Psychiatry.* 2009; 166:467–75. [PubMed: 19223437]
46. Dinstei I, et al. Unreliable evoked responses in autism. *Neuron.* 2012; 75:981–91. [PubMed: 22998867]
47. Pellicano E, Rhodes G, Calder AJ. Reduced gaze aftereffects are related to difficulties categorising gaze direction in children with autism. *Neuropsychologia.* 2013; 51:1504–9. [PubMed: 23583965]
48. Ethridge LE, et al. Reduced habituation of auditory evoked potentials indicate cortical hyper-excitability in Fragile X Syndrome. *Transl Psychiatry.* 2016; 6:e787. [PubMed: 27093069]
49. Cascio CJ, Woynaroski T, Baranek GT, Wallace MT. Toward an interdisciplinary approach to understanding sensory function in autism spectrum disorder. *Autism Res.* 2016; 9:920–5. [PubMed: 27090878]
50. Ramaswami M. Network plasticity in adaptive filtering and behavioral habituation. *Neuron.* 2014; 82:1216–29. [PubMed: 24945768]
51. Tartaglia M, et al. Mutations in PTPN11, encoding the protein tyrosine phosphatase SHP-2, cause Noonan syndrome. *Nat Genet.* 2001; 29:465–8. [PubMed: 11704759]
52. Iossifov I, et al. Low load for disruptive mutations in autism genes and their biased transmission. *Proc Natl Acad Sci U S A.* 2015; 112:E5600–7. [PubMed: 26401017]
53. Sugiura N, Patel RG, Corriveau RA. N-methyl-D-aspartate receptors regulate a group of transiently expressed genes in the developing brain. *J Biol Chem.* 2001; 276:14257–63. [PubMed: 11297529]

54. Myklebust LM, et al. Biochemical and cellular analysis of Ogden syndrome reveals downstream Nt-acetylation defects. *Hum Mol Genet.* 2015; 24:1956–76. [PubMed: 25489052]
55. Homsy J, et al. De novo mutations in congenital heart disease with neurodevelopmental and other congenital anomalies. *Science.* 2015; 350:1262–1266. [PubMed: 26785492]
56. van Bokhoven H. Genetic and epigenetic networks in intellectual disabilities. *Annu Rev Genet.* 2011; 45:81–104. [PubMed: 21910631]
57. Zhu T, et al. Histone methyltransferase Ash1L mediates activity-dependent repression of neurexin-1alpha. *Sci Rep.* 2016; 6:26597. [PubMed: 27229316]
58. Griswold AJ, et al. Targeted massively parallel sequencing of autism spectrum disorder-associated genes in a case control cohort reveals rare loss-of-function risk variants. *Mol Autism.* 2015; 6:43. [PubMed: 26185613]
59. Rhodes CT, et al. Cross-species Analyses Unravel the Complexity of H3K27me3 and H4K20me3 in the Context of Neural Stem Progenitor Cells. *Neuroepigenetics.* 2016; 6:10–25. [PubMed: 27429906]
60. Courchesne E, et al. Unusual brain growth patterns in early life in patients with autistic disorder: an MRI study. *Neurology.* 2001; 57:245–54. [PubMed: 11468308]
61. Shen MD, et al. Early brain enlargement and elevated extra-axial fluid in infants who develop autism spectrum disorder. *Brain.* 2013; 136:2825–35. [PubMed: 23838695]
62. Schumann CM, et al. Longitudinal magnetic resonance imaging study of cortical development through early childhood in autism. *J Neurosci.* 2010; 30:4419–27. [PubMed: 20335478]
63. Redcay E, Courchesne E. When is the brain enlarged in autism? A meta-analysis of all brain size reports. *Biol Psychiatry.* 2005; 58:1–9. [PubMed: 15935993]
64. Marchetto MC, et al. Altered proliferation and networks in neural cells derived from idiopathic autistic individuals. *Mol Psychiatry.* 2016
65. Sugathan A, et al. CHD8 regulates neurodevelopmental pathways associated with autism spectrum disorder in neural progenitors. *Proc Natl Acad Sci U S A.* 2014; 111:E4468–77. [PubMed: 25294932]
66. Cotney J, et al. The autism-associated chromatin modifier CHD8 regulates other autism risk genes during human neurodevelopment. *Nat Commun.* 2015; 6:6404. [PubMed: 25752243]
67. Courchesne E, et al. Neuron number and size in prefrontal cortex of children with autism. *JAMA.* 2011; 306:2001–10. [PubMed: 22068992]
68. Stoner R, et al. Patches of disorganization in the neocortex of children with autism. *N Engl J Med.* 2014; 370:1209–19. [PubMed: 24670167]
69. Chow ML, et al. Age-dependent brain gene expression and copy number anomalies in autism suggest distinct pathological processes at young versus mature ages. *PLoS Genet.* 2012; 8:e1002592. [PubMed: 22457638]
70. Pramparo T, et al. Cell cycle networks link gene expression dysregulation, mutation, and brain maldevelopment in autistic toddlers. *Mol Syst Biol.* 2015; 11:841. [PubMed: 26668231]
71. Geschwind DH, et al. The autism genetic resource exchange: a resource for the study of autism and related neuropsychiatric conditions. *Am J Hum Genet.* 2001; 69:463–6. [PubMed: 11452364]
72. Buxbaum JD, et al. The Autism Simplex Collection: an international, expertly phenotyped autism sample for genetic and phenotypic analyses. *Mol Autism.* 2014; 5:34. [PubMed: 25392729]
73. Ardlie KG, et al. The Genotype-Tissue Expression (GTEx) pilot analysis: Multitissue gene regulation in humans. *Science.* 2015; 348:648–660. [PubMed: 25954001]
74. Kircher M, et al. A general framework for estimating the relative pathogenicity of human genetic variants. *Nat Genet.* 2014; 46:310–5. [PubMed: 24487276]
75. Lek M, et al. Analysis of protein-coding genetic variation in 60,706 humans. *Nature.* 2016; 536:285–91. [PubMed: 27535533]
76. Feenstra I, et al. Balanced into array: genome-wide array analysis in 54 patients with an apparently balanced de novo chromosome rearrangement and a meta-analysis. *Eur J Hum Genet.* 2011; 19:1152–60. [PubMed: 21712853]
77. Vulto-van Silfhout AT, et al. Clinical significance of de novo and inherited copy-number variation. *Hum Mutat.* 2013; 34:1679–87. [PubMed: 24038936]

94. de Vries BB, et al. Clinical studies on submicroscopic subtelomeric rearrangements: a checklist. *J Med Genet.* 2001; 38:145–50. [PubMed: 11238680]
95. Lord, C., Rutter, M., DiLavore, PC., Risi, S. Autism Diagnostic Observation Schedule. Western Psychological Services; 2001.
96. Lord C, Rutter M, Le Couteur A. Autism Diagnostic Interview-Revised: a revised version of a diagnostic interview for caregivers of individuals with possible pervasive developmental disorders. *J Autism Dev Disord.* 1994; 24:659–85. [PubMed: 7814313]
97. Elliott, CD. Differential Ability Scales (2nd ed.): Introductory and technical manual. Harcourt Assessment; San Antonio, TX: 2007.
98. Fischbach GD, Lord C. The Simons Simplex Collection: a resource for identification of autism genetic risk factors. *Neuron.* 2010; 68:192–5. [PubMed: 20955926]
99. Pescosolido MF, et al. Expansion of the clinical phenotype associated with mutations in activity-dependent neuroprotective protein. *J Med Genet.* 2014; 51:587–9. [PubMed: 25057125]
100. Hoyer J, et al. Haploinsufficiency of ARID1B, a member of the SWI/SNF-a chromatin-remodeling complex, is a frequent cause of intellectual disability. *Am J Hum Genet.* 2012; 90:565–72. [PubMed: 22405089]
101. Epi KC, et al. De novo mutations in epileptic encephalopathies. *Nature.* 2013; 501:217–21. [PubMed: 23934111]
102. Merner N, et al. A de novo frameshift mutation in chromodomain helicase DNA-binding domain 8 (CHD8): A case report and literature review. *Am J Med Genet A.* 2016; 170A:1225–35. [PubMed: 26789910]
103. Kuechler A, et al. De novo mutations in beta-catenin (CTNNB1) appear to be a frequent cause of intellectual disability: expanding the mutational and clinical spectrum. *Human Genetics.* 2015; 134:97–109. [PubMed: 25326669]
104. Tucci V, et al. Dominant beta-catenin mutations cause intellectual disability with recognizable syndromic features. *J Clin Invest.* 2014; 124:1468–82. [PubMed: 24614104]
105. Winczewska-Wiktor A, et al. A de novo CTNNB1 nonsense mutation associated with syndromic atypical hyperekplexia, microcephaly and intellectual disability: a case report. *BMC Neurol.* 2016; 16:35. [PubMed: 26968164]
106. Lozano R, Vino A, Lozano C, Fisher SE, Deriziotis P. A de novo FOXP1 variant in a patient with autism, intellectual disability and severe speech and language impairment. *Eur J Hum Genet.* 2015; 23:1702–7. [PubMed: 25853299]
107. Sollis E, et al. Identification and functional characterization of de novo FOXP1 variants provides novel insights into the etiology of neurodevelopmental disorder. *Hum Mol Genet.* 2016; 25:546–57. [PubMed: 26647308]
108. Adams DR, et al. Three rare diseases in one Sib pair: RAI1, PCK1, GRIN2B mutations associated with Smith-Magenis Syndrome, cytosolic PEPCK deficiency and NMDA receptor glutamate insensitivity. *Mol Genet Metab.* 2014; 113:161–70. [PubMed: 24863970]
109. Endele S, et al. Mutations in GRIN2A and GRIN2B encoding regulatory subunits of NMDA receptors cause variable neurodevelopmental phenotypes. *Nat Genet.* 2010; 42:1021–6. [PubMed: 20890276]
110. Freunsch I, et al. Behavioral phenotype in five individuals with de novo mutations within the GRIN2B gene. *Behav Brain Funct.* 2013; 9:20. [PubMed: 23718928]
111. Lemke JR, et al. GRIN2B mutations in West syndrome and intellectual disability with focal epilepsy. *Ann Neurol.* 2014; 75:147–54. [PubMed: 24272827]
112. Cafiero C, et al. Novel de novo heterozygous loss-of-function variants in MED13L and further delineation of the MED13L haploinsufficiency syndrome. *Eur J Hum Genet.* 2015; 23:1499–504. [PubMed: 25712080]
113. van Haelst MM, et al. Further confirmation of the MED13L haploinsufficiency syndrome. *Eur J Hum Genet.* 2015; 23:135–8. [PubMed: 24781760]
114. Fukai R, et al. A case of autism spectrum disorder arising from a de novo missense mutation in POGZ. *J Hum Genet.* 2015; 60:277–9. [PubMed: 25694107]
115. White J, et al. POGZ truncating alleles cause syndromic intellectual disability. *Genome Med.* 2016; 8:3. [PubMed: 26739615]

116. Busa T, et al. Clinical presentation of PTEN mutations in childhood in the absence of family history of Cowden syndrome. *Eur J Paediatr Neurol.* 2015; 19:188–92. [PubMed: 25549896]
117. Buxbaum JD, et al. Mutation screening of the PTEN gene in patients with autism spectrum disorders and macrocephaly. *Am J Med Genet B Neuropsychiatr Genet.* 2007; 144B:484–91. [PubMed: 17427195]
118. Baasch AL, et al. Exome sequencing identifies a de novo SCN2A mutation in a patient with intractable seizures, severe intellectual disability, optic atrophy, muscular hypotonia, and brain abnormalities. *Epilepsia.* 2014; 55:e25–9. [PubMed: 24579881]
119. Dhamija R, Wirrell E, Falcao G, Kirmani S, Wong-Kisiel LC. Novel de novo SCN2A mutation in a child with migrating focal seizures of infancy. *Pediatr Neurol.* 2013; 49:486–8. [PubMed: 23988467]
120. Dimassi S, et al. Whole-exome sequencing improves the diagnosis yield in sporadic infantile spasm syndrome. *Clin Genet.* 2016; 89:198–204. [PubMed: 26138355]
121. Nakamura K, et al. Clinical spectrum of SCN2A mutations expanding to Ohtahara syndrome. *Neurology.* 2013; 81:992–8. [PubMed: 23935176]
122. Tavassoli T, et al. De novo SCN2A splice site mutation in a boy with Autism spectrum disorder. *BMC Med Genet.* 2014; 15:35. [PubMed: 24650168]
123. Herenger Y, et al. Long term follow up of two independent patients with Schinzel-Giedion carrying SETBP1 mutations. *Eur J Med Genet.* 2015; 58:479–87. [PubMed: 26188272]
124. Miyake F, et al. West syndrome in a patient with Schinzel-Giedion syndrome. *J Child Neurol.* 2015; 30:932–6. [PubMed: 25028416]
125. Takeuchi A, et al. Progressive brain atrophy in Schinzel-Giedion syndrome with a SETBP1 mutation. *Eur J Med Genet.* 2015; 58:369–71. [PubMed: 26096993]
126. Stamberger H, et al. STXBPI encephalopathy: A neurodevelopmental disorder including epilepsy. *Neurology.* 2016; 86:954–62. [PubMed: 26865513]
127. Heinen CA, et al. A specific mutation in TBL1XR1 causes Pierpont syndrome. *J Med Genet.* 2016; 53:330–7. [PubMed: 26769062]
128. Keshava Prasad TS, et al. Human Protein Reference Database--2009 update. *Nucleic Acids Res.* 2009; 37:D767–72. [PubMed: 18988627]
129. Szklarczyk D, et al. The STRING database in 2011: functional interaction networks of proteins, globally integrated and scored. *Nucleic Acids Res.* 2011; 39:D561–8. [PubMed: 21045058]
130. Wheeler DL, et al. Database resources of the National Center for Biotechnology. *Nucleic Acids Res.* 2003; 31:28–33. [PubMed: 12519941]
131. Attrill H, et al. FlyBase: establishing a Gene Group resource for *Drosophila melanogaster*. *Nucleic Acids Res.* 2016; 44:D786–92. [PubMed: 26467478]
132. Brand AH, Perrimon N. Targeted gene expression as a means of altering cell fates and generating dominant phenotypes. *Development.* 1993; 118:401–15. [PubMed: 8223268]
133. Dietzl G, et al. A genome-wide transgenic RNAi library for conditional gene inactivation in *Drosophila*. *Nature.* 2007; 448:151–6. [PubMed: 17625558]
134. Oortveld MA, et al. Human intellectual disability genes form conserved functional modules in *Drosophila*. *PLoS Genet.* 2013; 9:e1003911. [PubMed: 24204314]
135. Green EW, Fedele G, Giorgini F, Kyriacou CP. A *Drosophila* RNAi collection is subject to dominant phenotypic effects. *Nat Methods.* 2014; 11:222–3. [PubMed: 24577271]
136. Vissers JH, Manning SA, Kulkarni A, Harvey KF. A *Drosophila* RNAi library modulates Hippo pathway-dependent tissue growth. *Nat Commun.* 2016; 7:10368. [PubMed: 26758424]
137. Kramer JM, et al. Epigenetic regulation of learning and memory by *Drosophila* EHMT/G9a. *PLoS Biol.* 2011; 9:e1000569. [PubMed: 21245904]
138. Schindelin J, et al. Fiji: an open-source platform for biological-image analysis. *Nat Methods.* 2012; 9:676–82. [PubMed: 22743772]
139. Nijhof B, et al. A New Fiji-Based Algorithm That Systematically Quantifies Nine Synaptic Parameters Provides Insights into *Drosophila* NMJ Morphometry. *PLoS Comput Biol.* 2016; 12:e1004823. [PubMed: 26998933]



Figure 1. ASID patient network

13,475 probands with a primary diagnosis of ASD, ID, or DD collected from 15 international groups were screened using smMIPs. Circle size corresponds to the number of samples screened for each cohort. Cohort numbers (1–15) correspond to Supplementary Table 8.

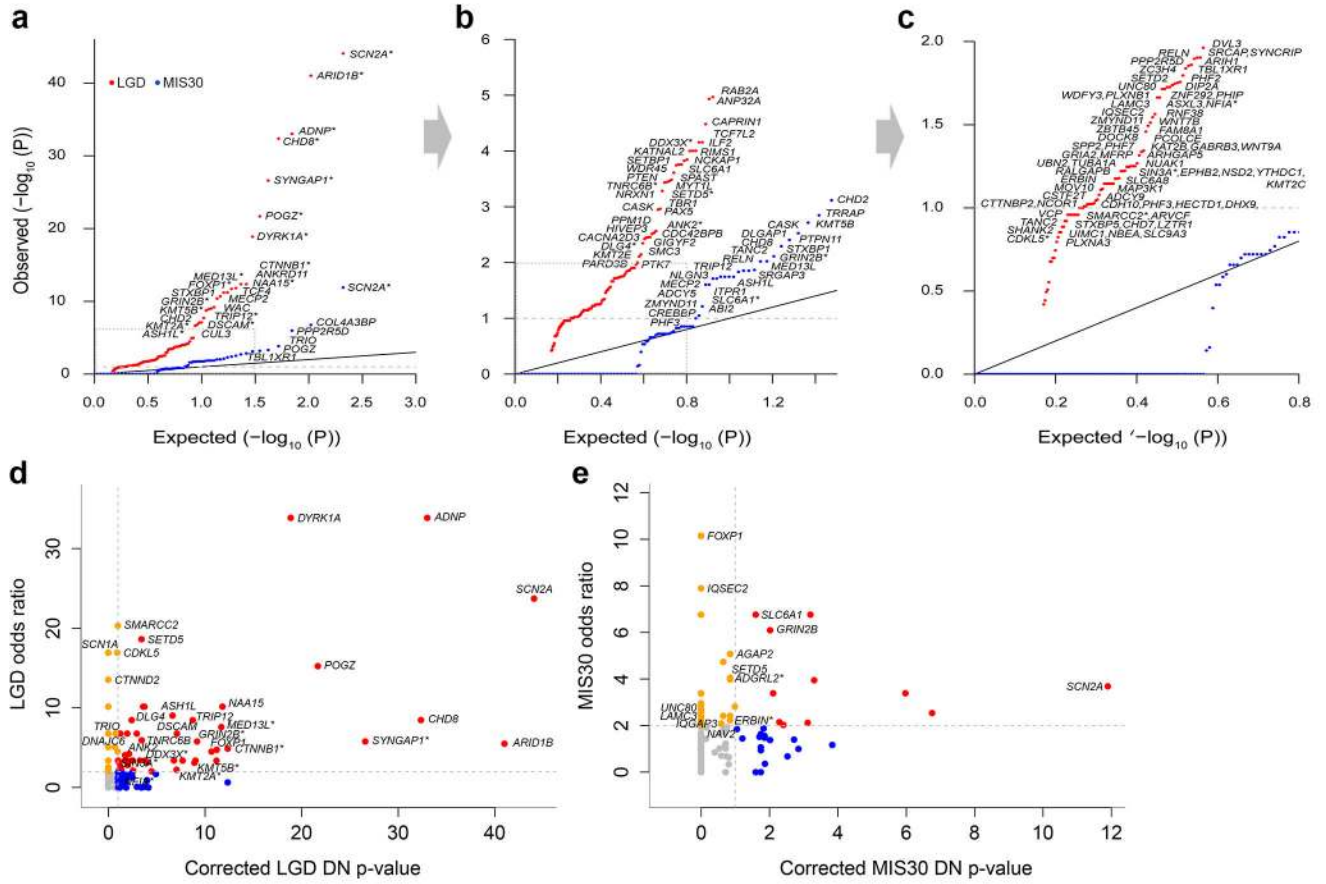


Figure 2. Targeted sequencing highlights genes that reach significance for DN mutations and private disruptive variant burden

(a–c) Quantile-quantile plots comparing the probability (FDR-corrected, inverse log transformed) of recurrent DN mutation for individual genes among proband samples compared to a uniform distribution given the number of genes tested (dashed gray line = significance threshold). Black dashed box (panels (a) and (b)) are zoomed in (panels (b) and (c), respectively). *Genes that reached significance for mutation burden. (d–e) Scatterplots depict the odds ratio (OR) for private variants compared to unaffected controls from ExAC (y-axis) versus the FDR-corrected DN p-value (x-axis; values have been inverse log transformed for plotting) by gene. Gray lines indicate the significance threshold for the DN p-value (horizontal) and an OR of two (vertical). Genes are classified as DN significant and OR > 2 (red dots), OR > 2 only (orange), and those that show a significant DN p-value only (blue). Gene name labels indicate a significant burden (FDR $q < 0.1$, simulation test) of either private LGD (d) or MIS30 (e) mutations in probands (Table 2; Methods). *Genes in which no control counts were observed where the 95% lower confidence bound was used as the most conservative OR estimate. See Supplementary Table 14 for underlying data.

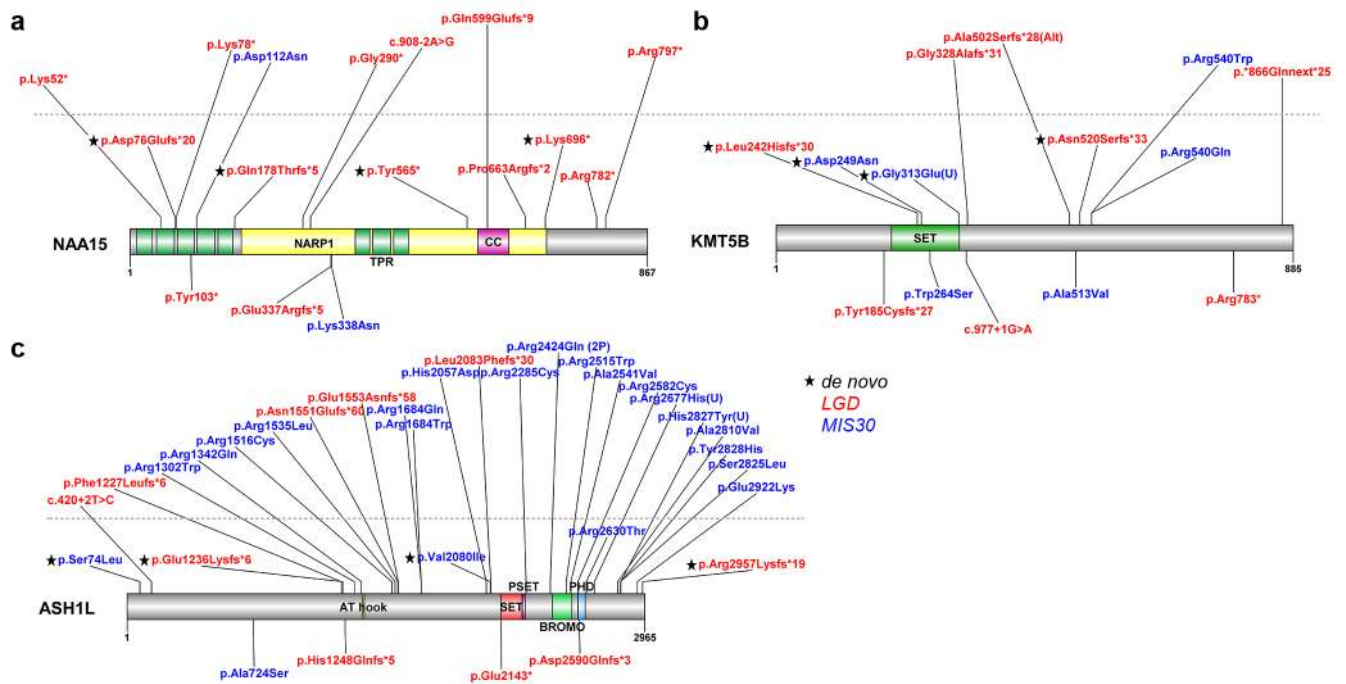


Figure 3. Protein location of private disruptive variants in new NDD candidate risk genes (a–c) Protein diagrams of (a) NAA15, (b) KMT5B, and (c) ASH1L with novel private LGD and MIS30 mutations identified in this study and published DN variants indicated in HGVS format. Annotated protein domains are shown (colored blocks) for the largest protein isoforms. Previously published DN variants (below protein structure, Supplementary Table 2) are compared to new variants in this study (above). Variants above the dashed line are of unknown inheritance; variants below the line have been validated for inheritance. Domain abbreviations: NARP1, NMDA receptor-regulated protein 1; CC, coiled coil; TRP, tetratricopeptide repeat region; PHD, plant homeodomain.

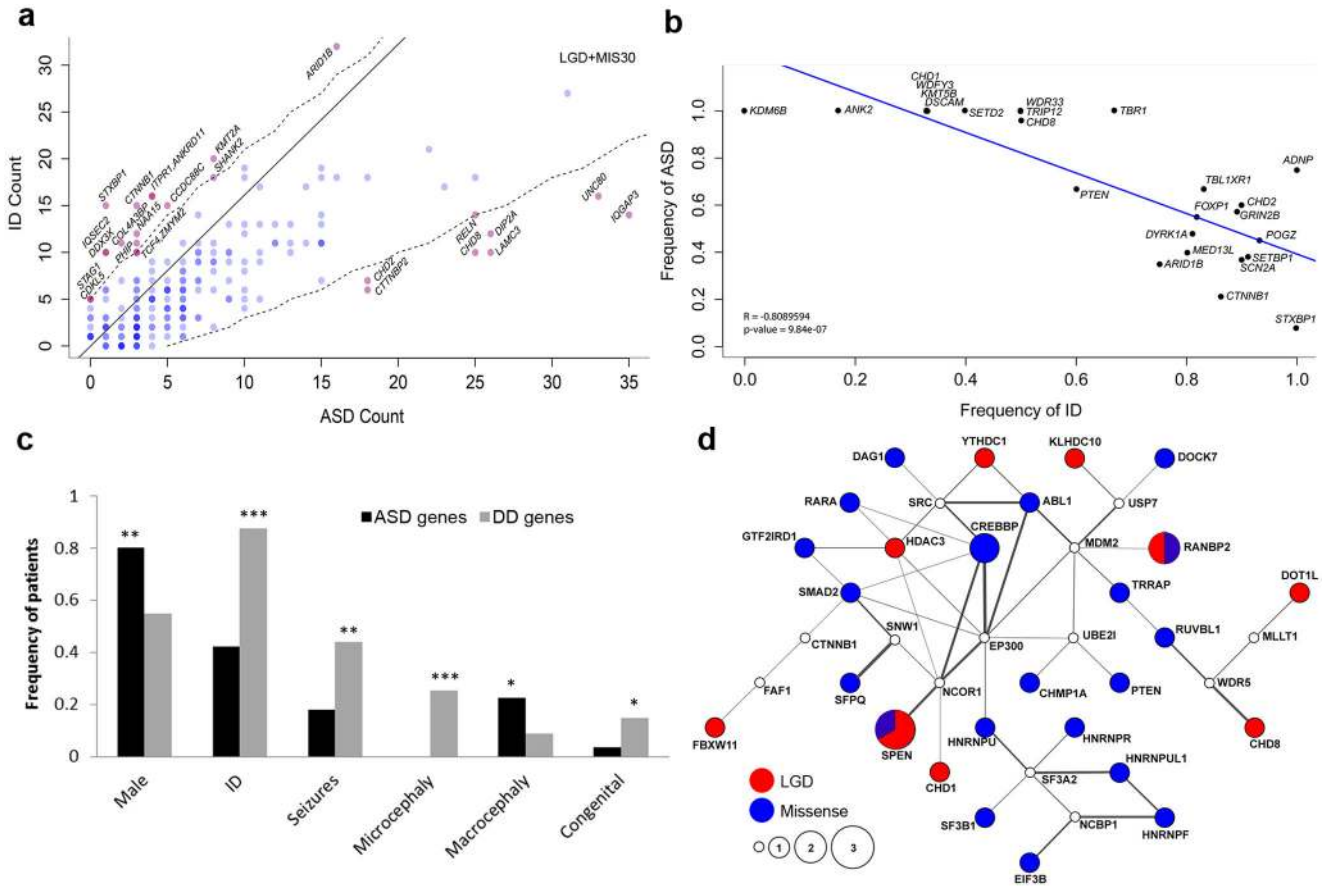


Figure 4. ASD versus ID genes

(a) Probands were categorized based on primary ascertainment either ASD or ID (including DD) and the combined number of LGD and MIS30 events per gene (published and this study) shown. Genes were tested for a bias to one phenotype (ASD or ID) by two one-tailed binomial tests ($p < 0.025$ for either bias). The solid line indicates equal proportions of mutations corrected for the screened population size. Significantly biased genes (red) are indicated with respect to the threshold (dashed line) and insignificant genes (blue). Darker shades of red or blue indicate multiple genes. (b) Scatterplot shows a negative correlation (Pearson's correlation) between ASD and ID diagnosis by gene (Table 3). (c) Bar graph compares phenotypic features of patients where genes are associated primarily with ASD diagnosis (>95%, black bars) compared to all other genes (gray bars) in Table 3. Significance was calculated by Fisher's two-tailed exact test, and p-values were FDR corrected. Exact p values: seizures ($p = 1.20 \times 10^{-4}$), congenital abnormalities ($p = 1.88 \times 10^{-2}$), microcephaly ($p = 1.79 \times 10^{-7}$), macrocephaly ($p = 5.25 \times 10^{-3}$), males ($p = 1.65 \times 10^{-4}$). * $p < 0.05$, ** $p < 0.001$, *** $p < 0.0001$. (d) SSC probands with ASD and an FSIQ > 100 were selected for pathway enrichment. Node size indicates the mutation score (calculated by MAGI based upon the number of DN mutations), and the color of the node indicates the number of DN LGD (red) and DN missense (no CADD cut-off; blue) mutations have been observed in affected probands, respectively. For *SPEN*, 2 LGD and 1 missense mutation have been observed and for *RANBP2*, 1 LGD and 1 missense mutation. White nodes indicate no DN mutations have been observed. Gray lines connect genes with

both protein-protein interactions and brain co-expression (Pearson's correlation coefficient $r^2 > 0.37$, Methods). Thicker lines correspond to more highly co-expressed gene pairs.

Author Manuscript

Author Manuscript

Author Manuscript

Author Manuscript

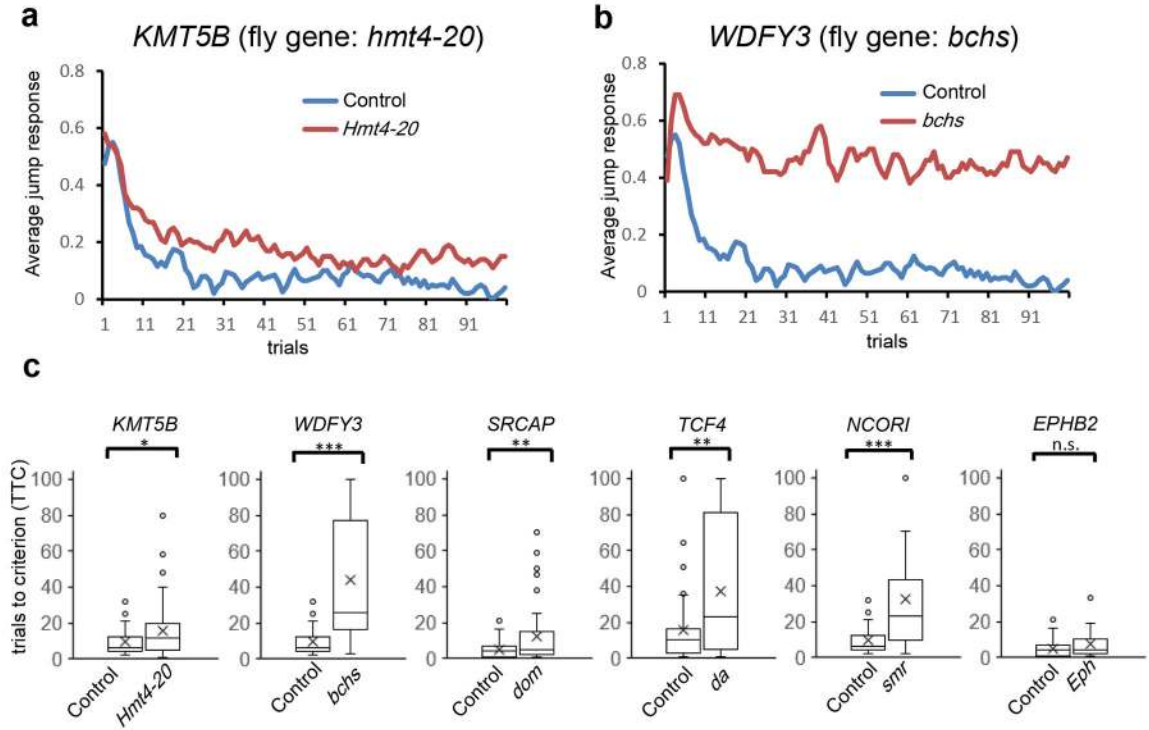


Figure 5. Habituation deficits in *Drosophila* knockdown models

(a–b) Representative jump response curves for (a) *hmt4-20* (ortholog of *KMT5B*) and (b) *bchs* (ortholog of *WDFY3*) panneuronal knockdown flies. The ratios of flies that responded to light-off stimuli are plotted over 100 trials (64 individual flies were tested for each genotype). Controls are plotted in blue and knockdowns are plotted in red. (c) Distribution of trials to no-jump criterion (TTC, Methods) of knockdowns versus corresponding control flies are plotted (cross, mean; middle line, median; box boundaries, upper and lower quartile; end of whiskers, maximum and minimum; dots, outliers). * $p < 0.05$, ** $p < 0.01$, *** $p < 0.001$ (linear regression model; 64 flies tested for each genotype; exact p values in Supplementary Table 23).

Table 1

Genes that reach *de novo* (DN) significance.

Gene	smMIP screening		Published exomes		Total		FDR-corrected DN p-value α		Study	
	DN LGD	DN MIS30	Probands screened	DN LGD	DN MIS30	Probands screened	DN LGD	DN MIS30		
<i>SCN2A</i>	10	1	13407	11	6	5237	21	7	1.27E-12	GOLD
<i>CHD8</i>	5	0	13407	12	2	6158	17	2	4.26E-33	GOLD
<i>POGZ</i>	4	1	13407	5	1	5237	9	2	2.06E-22	GOLD
<i>MED13L</i>	2	0	13407	6	2	6158	8	2	1.98E-12	GOLD
<i>STXBPI</i>	1	0	13407	5	2	6158	6	2	2.03E-11	GOLD
<i>GRIN2B</i>	2	1	13407	4	1	6158	6	2	6.39E-10	GOLD
<i>KMT5B</i>	2	1	12192	3	1	5237	5	2	1.21E-09	ASD4
<i>TRIP12</i>	2	0	13407	4	2	6158	6	2	1.84E-09	GOLD
<i>CHD2</i>	0	3	13407	7	1	6158	7	4	1.98E-08	GOLD
<i>ASHIL</i>	2	2	13407	3	0	5237	5	2	2.26E-07	GOLD
<i>SLC6A1</i>	2	0	13407	1	2	6158	3	2	1.75E-04	GOLD
<i>CASK</i>	0	0	12192	2	2	5237	2	2	1.09E-03	ASD4
<i>RELN</i>	2	1	13407	1	2	5237	3	3	1.27E-02	GOLD
<i>ARID1B</i>	6	0	13407	16	0	5237	22	0	9.84E-42	GOLD
<i>ADNP</i>	7	0	13407	9	0	6158	16	0	9.57E-34	GOLD
<i>SYNGAPI</i>	1	0	13407	16	1	6158	17	1	2.52E-27	GOLD
<i>DYRK1A</i>	2	0	13407	8	0	6158	10	0	1.32E-19	GOLD
<i>CTNNB1</i>	0	0	13407	7	0	6158	7	0	4.34E-13	GOLD
<i>ANKRD11</i>	0	0	12192	10	0	5237	10	0	4.34E-13	ASD5
<i>NAAI5</i>	4	0	12192	2	0	5237	6	0	1.52E-12	ASD4
<i>FOXP1</i>	2	0	13407	4	0	5237	6	0	5.90E-12	GOLD
<i>TCF4</i>	4	0	12192	3	1	5237	7	1	6.26E-12	ASD4
<i>MECP2</i>	2	0	11731	3	1	5237	5	1	4.12E-11	ASD6
<i>WAC</i>	1	0	13407	4	0	6158	5	0	9.63E-10	GOLD
<i>DSCAM</i>	2	0	13407	4	0	6158	6	0	7.89E-08	GOLD
<i>KMT2A</i>	0	0	11731	6	0	5237	6	0	8.57E-08	ASD6
<i>CUL3</i>	2	0	13407	2	0	5237	4	0	1.63E-07	GOLD

Gene	smMIP screening			Published exomes			Total			FDR-corrected DN p-value ^a			Study
	DN LGD	DN MIS30	Probands screened	DN LGD	DN MIS30	Probands screened	DN LGD	DN MIS30	Probands screened	DN LGD	DN MIS30	Probands screened	
<i>TCF7L2</i>	0	0	13407	3	0	6158	3	0	6158	0	0	6.97E-05	GOLD
<i>ILF2</i>	0	0	11731	2	0	5237	2	0	5237	0	0	7.01E-05	ASD6
<i>DDX3X</i>	0	0	13407	3	1	5237	3	1	5237	1	0.15	9.95E-05	GOLD
<i>RIMS1</i>	1	0	12192	2	0	5237	3	0	5237	0	1.00	9.95E-05	ASD4
<i>KATNAL2</i>	1	1	13407	2	0	5237	3	1	5237	1	0.19	1.00E-04	GOLD
<i>NCKAPI</i>	1	0	12192	2	0	6158	3	0	6158	0	1.00	1.43E-04	ASD5
<i>SETBP1</i>	0	0	13407	3	0	5237	3	0	5237	0	1.00	1.50E-04	GOLD
<i>WDR45</i>	0	0	11731	2	0	5237	2	0	5237	0	1.00	1.75E-04	ASD6
<i>SPAST</i>	0	0	12192	2	0	5237	2	0	5237	0	1.00	1.80E-04	ASD4
<i>PTEN</i>	0	0	13407	2	0	6158	2	0	6158	0	1.00	2.46E-04	GOLD
<i>MYT1L</i>	1	0	11731	2	0	6158	3	0	6158	0	1.00	3.29E-04	ASD6
<i>TNRC6B</i>	1	0	13407	2	0	5237	3	0	5237	0	1.00	3.49E-04	GOLD
<i>SETD5</i>	0	1	13407	3	0	6158	3	1	6158	0.14	0.14	3.61E-04	GOLD
<i>NRXN1</i>	0	0	11731	3	0	6158	3	0	6158	1.00	1.00	3.69E-04	ASD6
<i>TBR1</i>	0	0	13407	2	0	6158	2	0	6158	1.00	1.00	5.21E-04	GOLD
<i>PAX5</i>	0	0	13407	2	0	6158	2	0	6158	1.00	1.00	1.13E-03	GOLD
<i>PPM1D</i>	0	0	13407	2	0	6158	2	0	6158	1.00	1.00	2.73E-03	GOLD
<i>ANK2</i>	0	1	12192	4	1	5237	4	2	5237	0.19	0.19	2.93E-03	ASD5
<i>HIVEP3</i>	2	0	13407	1	0	5237	3	0	5237	1.00	1.00	3.07E-03	GOLD
<i>CDC42BPB</i>	0	0	12192	2	0	5237	2	0	5237	1.00	1.00	3.51E-03	ASD4
<i>CACNA2D3</i>	0	0	11731	2	0	5237	2	0	5237	1.00	1.00	3.54E-03	ASD6
<i>GIGYF2</i>	1	0	13407	1	0	5237	2	0	5237	1.00	1.00	3.57E-03	GOLD
<i>DLG4</i>	1	0	12192	1	0	5237	2	0	5237	1.00	1.00	3.77E-03	ASD5
<i>SMC3</i>	1	0	12192	1	1	5237	2	1	5237	0.19	0.19	4.51E-03	ASD4
<i>KMT2E</i>	0	0	12192	2	0	5237	2	0	5237	1.00	1.00	7.16E-03	ASD4
<i>PARD3B</i>	1	0	12192	1	0	5237	2	0	5237	1.00	1.00	7.79E-03	ASD5
<i>PTK7</i>	1	0	12192	1	0	5237	2	0	5237	1.00	1.00	9.99E-03	ASD4
<i>SRCAP</i>	1	0	12192	1	0	5237	2	0	5237	1.00	1.00	1.25E-02	ASD4
<i>PHF2</i>	0	0	12192	2	0	5237	2	0	5237	1.00	1.00	1.60E-02	ASD5
<i>ZC3H4</i>	0	0	13407	2	0	5237	2	0	5237	1.00	1.00	1.75E-02	GOLD

Gene	smMIP screening				Published exomes				Total				FDR-corrected DN p-value ^a	Study
	DN LGD	DN MIS30	Probands screened	DN LGD	DN MIS30	Probands screened	DN LGD	DN MIS30	Probands screened	DN LGD	DN MIS30	Probands screened		
<i>SETD2</i>	0	0	13407	2	0	5237	2	0	1.77E-02	1.00	GOLD			
<i>DIP2A</i>	0	0	13407	2	0	5237	2	0	1.79E-02	1.00	GOLD			
<i>UNC80</i>	1	0	12192	1	0	5237	2	0	1.83E-02	1.00	ASD5			
<i>ZNF292</i>	1	0	11731	1	0	5237	2	0	1.88E-02	1.00	ASD6			
<i>PHIP</i>	1	0	13407	1	0	5237	2	0	1.88E-02	1.00	GOLD			
<i>WDFY3*</i>	0	0	12192	2	0	5237	2	0	1.93E-02	1.00	ASD5			
<i>PLXNB1</i>	1	1	12192	1	0	5237	2	1	1.93E-02	0.40	ASD5			
<i>ASXL3</i>	0	0	11731	2	0	5237	2	0	2.17E-02	1.00	ASD6			
<i>LAMC3</i>	0	0	13407	2	0	5237	2	0	2.73E-02	1.00	GOLD			
<i>DOCK8</i>	1	0	11731	1	0	5237	2	0	5.40E-02	1.00	ASD6			
<i>KMT2C</i>	0	0	11731	2	0	5237	2	0	7.15E-02	1.00	ASD6			
<i>COL4A3BP</i>	0	0	13407	0	4	5237	0	4	1.00	1.75E-07	GOLD			
<i>PPP2R5D</i>	0	0	13407	1	3	6158	1	3	1.40E-02	1.04E-06	GOLD			
<i>TRIO</i>	0	1	13407	1	3	5237	1	4	0.18	1.44E-04	GOLD			
<i>TBL1XR1</i>	0	0	13407	1	2	6158	1	2	1.45E-02	6.37E-04	GOLD			
<i>PTPN11</i>	0	0	12192	0	2	5237	0	2	1.00	3.93E-03	ASD4			
<i>DLGAP1</i>	0	1	12192	0	1	5237	0	2	1.00	5.10E-03	ASD4			
<i>TANC2</i>	0	1	12192	1	1	5237	1	2	0.11	1.36E-02	ASD5			
<i>SRGAP3</i>	0	1	12192	0	1	5237	0	2	1.00	1.47E-02	ASD5			
<i>ITPR1</i>	0	1	11731	0	2	5237	0	3	1.00	1.80E-02	ASD6			
<i>ADCY5</i>	0	0	12192	0	2	5237	0	2	1.00	1.94E-02	ASD5			

* An LGD variant was identified in this gene using previously published smMIPs; therefore, the LGD count differs compared to Supplementary Table 11 to avoid duplicate counting.

^aFDR corrections were based on the number of samples for which parental DNA could be tested.

Table 2

Genes that carry a significant burden of private disruptive variation in cases.

Gene	LGD				MIS30			
	case count	control count	Corrected burden p-value	DN LGD significant	case count	control count	Corrected burden p-value	DN MIS30 significant
<i>SCN2A</i>	14	2	8.80E-05	YES	12	11	4.14E-02	YES
<i>GRIN2B</i>	8	0	2.26E-04	YES	9	5	3.66E-02	YES
<i>FOXP1</i>	7	5	5.84E-02	YES	6	2	4.34E-02	NO
<i>SETD5</i>	11	2	2.26E-04	YES	12	10	3.66E-02	NO
<i>ARID1B</i>	13	8	2.63E-03	YES	14	34	0.56	NO
<i>CHD8</i>	10	4	2.62E-03	YES	9	22	0.63	YES
<i>SYNGAP1</i>	8	0	2.26E-04	YES	3	10	0.90	NO
<i>ADNP</i>	10	1	2.20E-04	YES	1	3	0.92	NO
<i>DYRK1A</i>	10	1	2.20E-04	YES	3	8	0.83	NO
<i>MED13L</i>	10	0	8.80E-05	YES	7	16	0.63	YES
<i>POGZ</i>	9	2	1.32E-03	YES	7	6	0.15	YES
<i>NAAL5</i>	12	4	3.08E-04	YES	1	9	1.00	NO
<i>CTNNB1</i>	7	0	6.06E-04	YES	3	9	0.83	NO
<i>ASH1L</i>	8	3	7.04E-03	YES	17	35	0.35	YES
<i>DDX3X</i>	5	0	7.04E-03	YES	2	0	0.30	NO
<i>SMARCC2</i>	6	1	8.26E-03	NO	2	4	0.76	NO
<i>CTNND2</i>	4	1	7.04E-02	NO	8	31	0.98	NO
<i>SIN3A</i>	5	0	7.04E-03	NO	7	14	0.56	NO
<i>DSCAM</i>	6	3	4.76E-02	YES	12	39	0.83	NO
<i>SCN1A</i>	5	1	2.68E-02	NO	5	11	0.66	NO
<i>TNRC6B</i>	7	4	3.67E-02	YES	7	18	0.70	NO
<i>KMT2A</i>	4	0	2.68E-02	YES	3	9	0.83	NO
<i>TRIP12</i>	5	2	5.84E-02	YES	6	19	0.83	YES
<i>DLG4</i>	5	2	5.84E-02	YES	4	9	0.70	NO
<i>TRIO</i>	6	3	4.76E-02	NO	9	26	0.76	YES
<i>NFIA</i>	3	0	7.15E-02	NO	2	2	0.58	NO
<i>KMT5B</i>	5	0	7.04E-03	YES	3	0	0.13	YES

Gene	LGD						MIS30					
	case count	control count	Corrected burden p-value	DN LGD significant	case count	control count	Corrected burden p-value	DN MIS30 significant	case count	control count	Corrected burden p-value	DN MIS30 significant
<i>CDKL5</i>	5	1	2.68E-02	NO	0	0	NA	NO	0	NA	NO	NO
<i>DNAJC6</i>	6	4	7.28E-02	NO	10	15	0.30	NO	15	0.30	NO	NO
<i>ANK2</i>	9	9	7.04E-02	YES	21	58	0.62	YES	58	0.62	NO	NO
<i>IQSEC2</i>	2	0	0.20	NO	7	3	4.14E-02	NO	3	4.14E-02	NO	NO
<i>IQGAP3</i>	11	21	0.33	NO	21	34	9.87E-02	NO	34	9.87E-02	NO	NO
<i>SLC6A1</i>	1	0	0.48	YES	10	5	2.30E-02	YES	5	2.30E-02	YES	YES
<i>LAMC3</i>	8	19	0.53	YES	15	19	7.03E-02	YES	19	7.03E-02	NO	NO
<i>UNC80</i>	5	13	0.68	YES	30	38	1.21E-02	YES	38	1.21E-02	NO	NO
<i>ADGRLL2</i>	1	0	0.48	NO	6	0	1.21E-02	NO	0	1.21E-02	NO	NO
<i>ERBIN</i>	1	0	0.48	NO	4	0	4.34E-02	NO	0	4.34E-02	NO	NO
<i>NAV2</i>	1	9	1.00	NO	42	74	3.63E-02	NO	74	3.63E-02	NO	NO
<i>AGAP2</i>	0	2	1.00	NO	9	6	4.14E-02	NO	6	4.14E-02	NO	NO

P-values were calculated by simulating the number of private LGD or MIS30 events found in the study compared to 45,375 ExAC controls and were Benjamini-Hochberg corrected for the number of genes screened in the study where at least one private mutation was found in cases or controls (n = 176). Genes found in this table are labeled in Figure 2d-e. Corrected p-values < 0.1 were considered significant.

Table 3

Key phenotypic traits across participants with gene-disrupting mutations.

Gene	Total Cases	Cases evaluated in-depth	Mean Testing Age in months	Gender (% male)	Overall Severity		ASD	ID	Seizures	Microcephaly	Macrocephaly	Congenital Abnormality		VIQ β		NVIQ γ		ASD severity δ	
					modified Vries α	N						Rate	N	Rate	N	Rate	N	Rate	N
<i>KDM6B</i>	4	1	136	100%	2	100%	4	0%	4	0%	50%	4	0%	97.00	4	95.75	4	5.25	
<i>ANK2</i>	6	1	141	83%	2	100%	6	17%	6	0%	17%	6	17%	80.50	6	81.17	6	6.83	
<i>DSCAM</i>	3	2	133	100%	2	100%	3	33%	3	0%	33%	3	0%	71.33	3	55.33	3	9.00	
<i>KMT5B</i>	3	1	115	67%	1	100%	3	33%	3	0%	33%	3	0%	47.33	3	54.67	3	8.33	
<i>WDFY3</i>	3	2	181	100%	3	100%	3	33%	3	0%	67%	3	0%	57.33	3	77.00	3	8.00	
<i>CHD1</i>	3	1	123	100%	1	100%	3	33%	3	0%	0%	3	0%	83.00	3	97.67	3	7.00	
<i>SETD2</i>	5	2	190	60%	3	100%	4	40%	5	0%	40%	5	0%	100.67	3	94.67	3	7.67	
<i>WDR33</i>	2	1	129	100%	1	100%	2	50%	2	0%	0%	2	0%	67.00	1	66.00	2	8.50	
<i>TRIP12</i>	6	1	116	67%	2	100%	6	50%	6	0%	0%	6	0%	62.67	6	64.17	6	6.50	
<i>TBR1</i>	6	1	102	50%	2	100%	6	67%	6	0%	0%	6	0%	62.25	4	60.40	5	7.20	
<i>CHD8</i>	25	8	131	84%	11	96%	25	50%	24	0%	64%	25	0%	60.76	17	68.40	20	7.81	
<i>ADNP</i>	20	4	81	65%	14	75%	20	100%	20	10%	10%	19	44%	33.25	4	36.00	5	6.71	
<i>PTEN</i>	15	2	62	60%	6	67%	35	60%	15	0%	100%	15	8%	71.33	6	74.57	7	7.00	
<i>TBL1XR1</i>	13	1	139	54%	2	67%	6	83%	6	23%	15%	13	54%	52.33	3	55.00	3	6.00	
<i>CHD2</i>	12	4	134	50%	8	60%	10	90%	12	10%	10%	10	25%	71.33	6	63.33	6	8.17	
<i>GRIN2B</i>	22	3	146	55%	8	57%	14	89%	21	16%	5%	19	13%	58.00	6	56.83	6	8.17	
<i>FOXP1</i>	11	2	160	64%	9	55%	11	82%	11	0%	33%	9	20%	53.50	2	48.00	2	7.50	
<i>DYRK1A</i>	21	6	195	57%	17	48%	21	81%	21	90%	0%	21	33%	44.29	7	51.57	7	7.43	
<i>POGZ</i>	44	1	109	57%	24	45%	44	93%	44	11%	5%	43	13%	72.20	5	68.80	5	8.60	
<i>MED13L</i>	15	1	112	53%	9	40%	10	80%	15	20%	7%	15	36%	57.33	3	73.67	3	6.67	
<i>SETBP1</i>	24	1	98	58%	5	38%	8	91%	24	9%	0%	11	18%	60.33	3	69.67	3	6.00	
<i>SCN2A</i>	55	2	75	53%	13	37%	35	90%	55	25%	2%	44	21%	52.38	8	57.25	8	6.50	
<i>ARID1B</i>	28	3	137	43%	22	35%	26	75%	28	7%	14%	28	21%	67.14	7	67.00	7	7.00	
<i>CTNNB1</i>	30	1	121	43%	21	21%	24	86%	30	75%	0%	28	31%	51.75	4	56.00	4	6.50	

Gene	Total Cases	Cases evaluated in-depth	Mean Testing Age in months	Gender (% male)	Overall Severity		ASD	ID	Seizures	Microcephaly	Macrocephaly	Congenital Abnormality		VIQ β	NVIQ γ	ASD severity δ					
					modified de Vries α	N						Rate	N			Rate	Mean	N	Mean	N	
STXBPI	49	1	107	51%	4.37	49	8%	49	100%	49	86%	49	8%	49	0%	49	30.00	30.00	3.00	1	1

In order to maximize the number of cases for each assessment, the number of cases considered for calculated variables differs. The N for each variable is listed.

α See Supplementary Table 22 for modified de Vries scoring criteria.

β Mean verbal IQ (VIQ) has a mean of 100 and standard deviation of 15.

γ Mean nonverbal IQ (NVIQ) has a mean of 100 and standard deviation of 15.

δ Mean ASD severity is derived from the ADOS-2 Calibrated Severity Score (CSS) and ranges from 1–10 with scores between 4–10 representing symptoms within ASD, with 10 being the most severe.